John Brown University

Development of a Low-Cost Maximum Power Point Tracker for Low-Wattage Photovoltaic Systems

SOLARIS
POWER SYSTEMS

FINAL REPORT

Kyle Crouse, Zach Lee, Austin Ricks, Zeke Zumbro

Professor Kim Cornett

May 5, 2015

ABSTRACT

The power obtained by photovoltaic panels typically is not the maximum power that could be produced by the panel. Maximum Power Point Trackers (MPPTs) have been developed in order to increase the power output of a panel by setting its operating point to the panel to the point where maximum power is extracted from the panel. The major issue with current Maximum Power Point Trackers is their high cost. The report outlines the design, assembly, and testing of a $91.32 prototype for a 65 W maximum power point tracker. Reasons for the design as well was market considerations are first discussed to justify the need for this design. Initial design parameters including technical and financial considerations are then outline for the project. The design of each subsystem, including the DC-DC converter, current and voltage sensors, algorithm, printed circuit board (PCB), and housing, are then discussed in detail. This design process includes the equations, diagrams and computer simulations used in the design process. Explanation of the construction and debugging process follows this design process. Included in this section is the creation of two small breakout boards, called stamps, which were used to correct errors in the original PCB. The report then outlines the methods used to test the MPPT, including subsystems testing and final design testing. From this testing it was determined that the circuit performed as expected when tested using a 15 W PV panel. From this testing an average power increase of 35.24%, which exceeded the design parameter of 10% power increase. Future work will include testing the design to its full rated power using a 65 W panel. However, all components are designed to exceed this power rating. Additional future work is also outlined, including increasing the efficiency of the DC-DC converter used in this design and decreasing the switching frequency used. A final production cost for 1000 units was calculated to be $40.66 which was below the desired final production cost of $75.

CONTENTS

FIGURES

TABLES

I. Introduction

Photovoltaic (PV) systems are an increasingly popular source of power today, as they can be completely independent of an electrical grid, produce no emissions, and require only the sun as a fuel source. These advantages also make PV systems a viable way to alleviate energy poverty in the developing world. However, those lacking access to a reliable energy are often prohibited by the initial cost required by such PV systems. The use of a maximum power point tracker (MPPT) for PV panels can decrease this initial cost by increasing the efficiency of each panel, thus necessitating fewer panels to achieve the required power budget.

While PV systems are widely recognized as an optimal source of power in developing countries, communities in these countries are yet faced with two issues regarding the implementation of such systems: 1) the power provided by PV systems is inadequate to fulfill the total need for a community, thus necessitating kerosene or other fossil fuels as supplemental power, or 2) the community lacks the necessary funds to make the initial investment for a PV system. A PV system typically consists of one or more PV panels connected to a battery. By introducing an MPPT into a PV system, the efficiency of each panel is optimized, increasing the power output relative to PV systems without maximum power point tracking. To a community presently possessing a PV system, adding an MPPT drastically increases the power produced by the system for the community, reducing the community's need for fossil fuels as supplemental power. To a community considering the purchase of PV panels, the addition of an MPPT reduces the initial investment required, as fewer panels are necessary to achieve the desired power budget.

This project fits within the Environmental Technology market segment. The target market for this project is home and business owners in the developed and developing world who utilize low-wattage PV systems to provide electricity and reduce their environmental impact. This project is primarily focused on consumers in the developing world who cannot afford MPPTs on the market today. Table I shows the current costs of MPPTs on the market today.

Table I. Commercial MPPT Prices

Name	*Max Power Intake (W)*	*Price ($)*
BZ Products MPPT250	300	111
Blue Sky 2512i	300	213
Morningstar SunSaver 15 Amp MPPT Solar Charge Controller	180	250
Rogue MPT-3048	360	350
Morningstar TriStar 30 Amp MPPT Solar Charge Controller	360	355

From Table I it can be seen that most MPPTs on the market today cost over $100, which is out of the price range of many in the developing world. A high priced MPPT makes the purchase of an additional panel more cost effective than adding an MPPT. This project seeks to develop a more affordable MPPT to meet this market need. This device will be important for this market as it decreases the cost per watt of PV systems by increasing the power output of a PV system at a lower cost than adding the equivalent capacity by adding additional PV panels. This device will thus help to provide access to affordable electricity in developing regions. The project will also have a broader market toward any PV user desiring to maximize the efficiency of his or her PV system at the lowest cost.

This report details the design, construction, and testing process of a low-cost MPPT appropriate for small PV systems in developing countries. The resulting MPPT is designed to receive as input a PV panel or array with a maximum capacity of 100 W. The MPPT which has been designed is extremely simple and does not include any additional features which would increase cost and add additional points of failure. The design is water resistant and robust against physical damage.

As a result of this project a working MPPT has been developed which has demonstrated the ability to increase the power to a resistive load by an average of 35.24%.The MPPT has been tested extensively with a 15 W PV panel and has been tested on a 65 W panel. Each subsystem of the MPPT has been thoroughly tested, including the DC-DC converter, current and voltage sensors, and housing. Although the initial design parameters were changed after consulting with Dr. Song, all of these new parameters were met with the exception of the efficiency standard for the DC-DC converter. It was found that the DC-DC converter for this design was 75% efficient which exceeded the initial requirements. A detailed user's manual as well as packaging have also been created for this project.

II. Problem Definition

MPPTs increase the power output of PV panels, however due to the high costs of many on the market they are not economically viable for small solar arrays; this creates a need for a lower cost option. The proposed project would decrease the cost of the MPPT to $75 by utilizing a low-cost microprocessor, low-cost sensing technologies, and by custom designing components as necessary. The MPPT will be designed with widely available, modular components, to allow for ease of maintenance and repair. Additionally, the MPPT will be designed to have a plug-and-play interface, so as to simplify installation and setup. As PV systems are necessarily outdoors, the MPPT will be housed in such a way as to withstand adverse weather conditions, such as rain and extreme temperatures.

A. Requirements Breakdown

The initial technical performance criteria for this project can be seen in Table II.

Table II. Technical Criteria

	Min	*Max*
V_{in}	5 V	38 V
V_{out}*	11.8 V	14.4 V
ΔV_{out}	-	2.5%
P	-	300 W
ΔP	+10%	-
Efficiency	90%	-
Self-Consumption	-	50 mW
Length	-	8"
Width	-	6"
Height	-	4"

After consulting with our mentor Dr. Ted Song, and doing preliminary research, these criteria were adjusted to more realistic levels for a one-semester undergraduate project. In addition, the load for the project was changed from a battery load to a resistive load. These new criteria can be seen in Table III.

Table III. Modified Technical Criteria

	Min	*Max*
V_{in}	5 V	40 V
V_{out}*	0 V	25 V
ΔV_{out}	-	N/A
P	-	100 W
ΔP	+10%	-
Efficiency	70%	-
Self-Consumption	-	100 mW
Length	-	8"
Width	-	6"
Height	-	4"

The criteria of V_{in} was determined based on the minimum and maximum voltage outputs for PV panels in the 100 W range. The criteria for V_{out} was determined based on realistic values for voltage across the output resistor when tracking the maximum power point. This is the type of battery system expected to be used by the target market, as it is an affordable energy

storage technology. The output voltage ripple was determined not be important for this design as the output voltage would fluctuate as the MPPT operated regardless of the output capacitor. However, for calculations to determine the output capacitor an allowable voltage ripple of 2.5% was used. The minimum ΔP criteria of +10% means that the MPPT should increase the power output of the panel by at least 10%. The purpose of the MPPT is to increase the power output of the PV panel, thus this minimum is an important criteria for determining the success of the design. The criteria for minimum efficiency of the DC-DC converter within the MPPT has been set to be 70%. The goal of a MPPT is the increase of efficiency of the PV system, thus inefficiencies within the DC-DC converter must be minimized. However, extremely efficient DC-DC converters are difficult to design and outside the scope of this one-semester project, so an allowable efficiency of 70% is realistic. The criteria for self-consumption, or the power taken to run the MPPT, will be less than 100 mW. This too is important because power used to run the controller and other components contributes to inefficiency of the MPPT, and thus should be minimized. Finally, the mechanical size constraint of 8" x 6" x 4" for the device was determined to reduce the footprint of the device where it is installed and to ensure that the device can be easily transported.

B. Constraints

1) *Production cost must not exceed $75*. As previously stated, a key goal for this project is to design an MPPT that is substantially lower in cost than comparable MPPTs on the market today, making this a primary constraint on the design.
2) *Prototype cost must not exceed $150*. Since electrical components and printed circuit board fabrication reduce significantly at production quantities, it is expected that the prototype will cost more than a production model of this MPPT. A $150 budget has been determined for this prototype based on the money provided by John Brown University as seed funding for this project.
3) *Prototype must be weather resistant*. PV panels are necessarily outdoors, thus making it highly likely that the MPPT will be outdoors as well. Without weather resistance, the MPPT will quickly break down and fail to function. The MPPT may be mounted inside of buildings to which power is supplied, but this is not guaranteed. In circumstances when this is not available, the product will be designed to be weather resistant.
4) *Design must prevent electric shock to users*. Users should not be shocked when installing the device, nor should technicians be shocked when servicing the device.
5) *Prototype must be completed by May 5*.

C. Testing Plan

In order to determine if the prototype conformed to the design requirements, tests were designed to analyze each subsystem as well as the system as a whole. Testing of the DC-DC

converter subsystem was done first in order to determine proper functionality and an acceptable efficiency. The operation of the DC-DC converter was tested by attaching the input side of the converter to a DC voltage source. An MSP430 was then will be used to provide pulse width modulation (PWM) waveform to the DC-DC converter. The output of the DC-DC converter was then measured across a load resistor using the Digital Multimeter (DMM). Success of the DC-DC converter was determined based on whether or not the output voltage was able to be controlled by the PWM signal provided by the AWG. The efficiency of the DC-DC converter was also tested by measuring the input voltage and current to the DC-DC converter using the DMM to find the input power. This was compared to the output power calculated using the load resistance and output voltage measured using the DMM. The circuit was determined to be successful if the efficiency was greater than 70%.

The controller subsystem was also tested. The first elements of the controller subsystem to be tested was the voltage and current sensors. Each sensor was evaluated by providing to it a known voltage or current using a DC voltage source and resistors. The output of the sensor was then compared to the reading from a DMM to determine if the output voltage of the sensor was linearly related to the input. The output of each sensor was then read using the MSP430 ADC. Linear regression was then used to relate the ADC values to the actual voltage and current values read by the DMMs.

The mechanical case subsystem was also tested. The case subsystem was primarily tested for weatherproofing. To do this the case was sealed and water will then be poured over the case in a way which simulated heavy rainfall. The case was then opened and examined to determine if water was able to penetrate the case. The casing was considered successful if no evidence of leakage is found after testing for 1 hour.

Finally the integrated system was tested. Temperature testing was conducted using the PCB circuit inside of the sealed housing. Two thermocouples were used to read temperature levels as the circuit was given power. Maximum temperatures of the individual circuit components were found from the data sheets. This indicated a maximum circuit temperature of 185°F. Testing results that produce an equilibrium temperature less than the 185°F maximum will be successful.

The effectiveness of the MPPT will be evaluated by determining the increase in power provided to the load when using the MPPT versus when a resistor is directly connected to the panel. The panels connected to MPPT and resistor will then be swapped so each is connected to each panel. The results of these tests will be compared to eliminate variations from different PV panels. The MPPT was considered successful if the average output power was at least 20% higher than the average output power of the PV panel connected directly to the load.

III. Technical Solution

A. Brainstorming of Multiple Ideas

The basic design of a MPPT has been well established, so there was no need to brainstorm alternatives to this design. However the subsystems of the design had many alternatives. There are six major subsystems for which brainstorming alternatives was necessary. The first of these was the DC-DC converter. Five alternatives for the DC-DC converter were determined based on the converters which were covering in EE3503 Power Electronics. These converters were Buck, Boost, Buck-Boost, Ćuk, and SEPIC. The next major subsystem was the algorithm. Based on previous research three alternatives were established. These were Perturb and Observe, Incremental Conductance, and Fractional Open Circuit Voltage. The next subsystem to be considered were sensors. For current sensors three options were considered; a shunt resistor, a Hall Effect current sensor, and a fiber optic current sensor. For voltage only two alternatives were available. These were using the microcontroller's ADC with a resistive divider, and using a voltage measurement integrated circuit. For the controller subsystem four alternatives were developed; an MSP430, a digital signal processor, an FPGA, and an Arduino.

The final subsystem for which alternatives were brainstormed was the housing. Ideas for housing material included printed ABS, purchased injection molding plastic enclosures, purchased extruded aluminum enclosures with outward facing fins, aluminum sheet metal, and purchased ammunition boxes. At the start, plastic was the favored material because it would be easier to work, would not heat up enough to burn the user, and would meet water-resistance and debris resistant requirements. However, aluminum was chosen because it is not difficult to machine, requires a significant amount of heat to burn the user that the circuit is not expected to produce, can be made to fit all durability requirements, and is able to conduct heat better than typical ABS plastic can. As for cable input and output into the housing, not a lot of valid ideas were thought of that would provide strain relief and weather resistance. The way coax cables are used was looked at as a reference but turned down for lack of application to the product concept. The next idea was to use cable glands, which use a double threaded shell of PVC and a nut that compresses a plastic and rubber bit onto the cable. For heat dissipation, the ideas looked at were vents in the bottom of the housing, a small fan to circulate interior air, and circuit components sinking heat directly into the enclosure wall. For mounting, the ideas were surface mounting, pole mounting, and solar array frame mounting. Finally, the alternatives to have a lid or not to have a lid were determined, including what type of lid attachment should be used. Attachment ideas included clamping using jar hooking clamps on all side or with a hinge on one side, a draw latch with hinge, or screws between the lid and box. Each subsystem was then analyzed to determine what criteria should be used to select each component. The components were then run through a decision matrix in order to determine which alternative would be used.

B. Selection of Design Ideas to Pursue

The decision matrix in Table IV outlines the selection of a DC-DC converter topology. Four criteria were developed to evaluate the five alternatives. These criteria were cost, simplicity, inversion, and flexibility. The cost criteria involves the costs of components needed for the DC-DC converter design as well as the size of the PCB required, as this will increase the total cost. A higher score in this category signifies a lower cost. The simplicity criteria involves how difficult the design will be as well as difficulty in controlling the converter. Simplicity scores are higher for designs which do not require driver ICs for high-side switching, as well as for designs with fewer components. The inversion criteria grants higher points to converters which do not invert the output. Finally, the flexibility criteria grants higher scores to converters which are able to handle inputs which are both higher and lower than the output and lower scores to converters which can only increase or only decrease voltages. The points in the total column are highest for the best design, which in this case is the SEPIC and Ćuk converters. Since cost was a prime factor, the Ćuk Converter was finally chosen for this design.

Table IV. DC-DC Converter Decision Matrix

DC-DC Converters	**Cost**	**Simplicity**	**Inversion**	**Flexibility**	Total
Buck	7	5	10	5	**20**
Boost	9	9	10	3	**22**
Buck-Boost	7	5	7	10	**22**
Cuk	5	7	7	10	**24**
SEPIC	3	6	10	10	**24**

The decision matrix in Table V outlines the selection of a MPPT algorithm for the design. Six criteria were developed to evaluate the three alternatives. These criteria were simplicity, required sensors, computational resources, effectiveness, speed, and flexibility. The simplicity criteria measures the ease with which the algorithm can be implemented in code. The simplicity score is highest for algorithms which are easily implemented and lowest for algorithms which are more difficult to implement. The required sensors criteria involves the number and types of sensors required for the algorithm. Perturb and Observe and Incremental Conductance both score poorly in this area because they require a current sensor and voltage sensor, while Fractional Open Circuit Voltage only requires a voltage sensor. The computational resources criteria measures how much processing power is needed to implement the algorithm. This is measured by the number of operations which are necessary in each loop. A higher score in this category represents fewer operations needed. The effectiveness criteria represents how accurately the algorithm find the correct maximum power point (MPP). This score is highest for the Incremental Conductance method which finds and latches on to the MPP. The Perturb and Observe algorithm is next highest since it

find the MPP but oscillates around it. Finally, the Fractional Open Circuit Voltage method is least effective as it only approximates the MPP. The speed criteria represents how quickly the algorithm is able to find the MPP. A higher score in speed means that the algorithm find the MPP faster. The flexibility criteria is rates the algorithms on their ability to work with different PV panels without calibration. Since the Fractional Open Circuit Voltage method relies on specifics about the panel, it scores poorly in this category, while the other two algorithms score well. From the total column in Table V it can be seen that the Perturb and Observe method is preferable, and thus this algorithm was chosen for this design.

Table V. Algorithms Decision Matrix

Algorithms	Simplicity	Required Sensors	Computational Resources	Effectiveness	Speed	Flexibility	**Total**
Perturb and Observe	8	6	9	9	8	10	**50**
Incremental Conductance	7	6	7	10	9	10	**49**
Fractional Open Circuit Voltage	10	10	10	6	10	2	**48**

The decision matrices in Table VI and Table VII outline the selection of current and voltage sensors for the design. The criteria for both matrices are the same: cost, simplicity, reliability, and efficiency. The cost criteria relates to the cost of the sensor or components to build the sensor. A higher score represents a lower cost. The simplicity criteria involves how difficult the sensor will be to design and implement, as well as the ease with which the sensor can be read by the controller. A higher simplicity score represents a simpler design. The accuracy criteria represents how accurate the sensor is relative to the actual value, with a higher accuracy score meaning that the sensor is more accurate. The efficiency criteria measures how much power is consumed by the sensor. A higher score in efficiency represents a lower power consumption for the sensor. From Table VI it can be seen the both the Shunt Resistor and Hall Effect sensor have the same total score. The Shunt Resistor and Amplifier has been selected however, due to greater simplicity. From Table VII it can be seen that the Microcontroller ADC with Voltage Divider method received the highest score and will be used for this project.

Table VI. Current Sensor Decision Matrix

Current Sensors	Cost	Simplicity	Accuracy	Efficiency	**Total**
Shunt Resistor and Amplifier	8	7	7	6	**27**
Hall Effect Current Sensor	7	4	8	8	**27**
Fiber Optic Current Sensor	1	1	10	8	**20**

Table VII. Voltage Sensor Decision Matrix

Voltage Sensor	Cost	Simplicity	Accuracy	Efficiency	**Total**
Microcontroller ADC and Voltage Divider	9	10	8	6	**34**
Voltage Measurement IC	7	7	9	9	**32**

The decision matrix in Table VIII outlines the selection of a controller. The criteria for controller selection are cost, processing power, ease of programming, power consumption, and peripherals. For the cost criteria, a higher score in the represents a lower cost. The processing power criteria represents the amount of processing power the controller has, such as its clock speed and the ability to perform tasks in parallel. High scores in this category represent high processing power. The ease of programing criteria takes into account the ease with which the algorithm can be implemented on the controller. This includes the language which is used to program the controller, development environments available to be used when programming the controller, and availability of sample code. High scores in ease of programming correspond to simpler implementation, a strong development environment, and access to sample code. The power consumption criteria takes into account how much power each controller would require. Since self-consumption of the MPPT has been limited to below 100 mW, it is important that power consumption of the controller be kept low. A high score in power consumption relates to a low power consumption. Finally, the peripherals criteria takes into account the presence of peripherals available on the controller, including ADCs, PWM generators, etc. High scores in this category were given to controllers with these peripherals. From the total column of Table VIII it can be seen that the MSP430 microcontroller received the highest score, and will be used as the controller for this project. This also aligns with the SURF grant which is providing additional funds for this project, as the grant specifies that an MSP430 be used.

Table VIII. Controller Decision Matrix

Controllers	Cost	Processing Power	Ease of Programming	Power Consumption	Peripherals	**Total**
MSP430	10	6	9	9	9	**43**
Digital Signal Processor	8	8	7	7	10	**40**
FPGA	4	9	7	5	8	**33**
Arduino	6	6	10	7	9	**38**

The criteria for housing of the printed circuit board include weather resistance, durability, and prevention of electrical shock to the user. Additional desired characteristics of the housing design include affordability, ease of manufacture, use of common materials to provide for simple and quick maintenance, reversible component attachments, adequate heat dissipation for the PCB, and durable mounting into the PV array circuit. Since the project is still in the design phase, alternatives that match these constraints and goals are not available and additional research will be made that will affect design choices in the future. Housing design manufacture is scheduled for 20 March 2015. Testing is scheduled for 12 April 2015, and the results will affect the final prototype design for final presentation on 5 May 2015.

At the time of proposal submission, plastic is the favored material for circuit housing to minimize cost and weight. Metal housing would heat up in the summer, hindering heat dissipation from the circuit, and would need to be properly sealed to prevent rust. A hinged lid with O-ring sealing is an alternative that would allow for ease of access to the circuit while keeping the circuit weather resistant. Additional research and future design alternatives will be included in the online project notebooks.

The criteria for housing of the printed circuit board include weather resistance, durability, and prevention of electrical shock to the user. Additional desired characteristics of the housing design include affordability, ease of manufacture, use of common materials to provide for simple and quick maintenance, reversible component attachments, adequate heat dissipation for the PCB, and durable mounting into the PV array circuit.

C. Technical Analysis & Design Details

1. Electrical Details

Technical analysis of the chosen design began by determining the DC-DC converter parameters needed in the design. These parameters can be seen in Table IX. The values in Table IX were selected based on PV panel characteristics as well as research into parameters of other comparable MPPTs.

Table IX. Converter Parameters

Parameter	Minimum	Maximum
Vs (V)	5	38
R (Ω)	1.44	7.5
D	0.24	0.75
f (kHz)	100	200
ΔVC1 (V)	-	0.1
ΔVC2 (V)		0.25

A Ćuk Converter topology was selected for the DC-DC converter. A diagram of the Ćuk topology can be seen in Fig. 1.

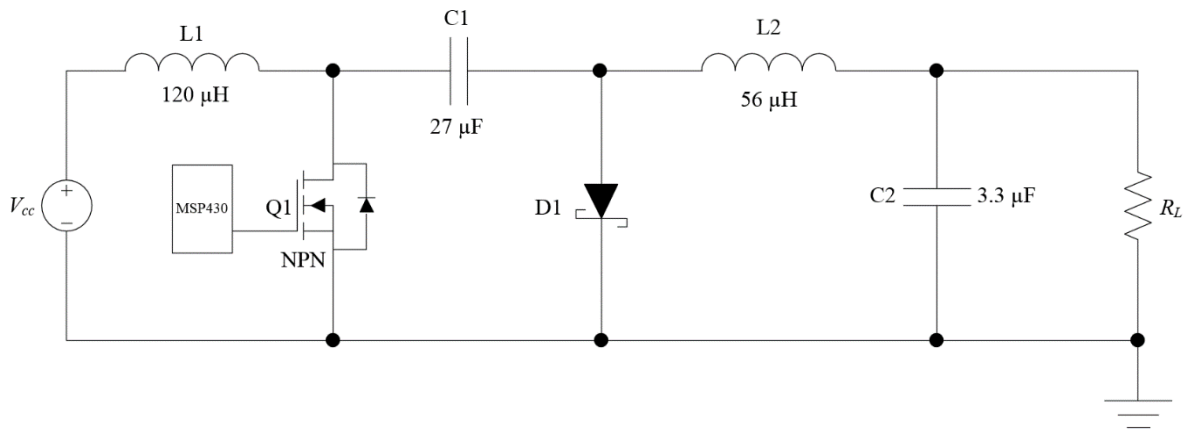

Fig. 1. Cuk Converter Topology

The values of L_1, L_2, C_1, C_2 were found using equations (1) through (4).

$$L_1 \geq \frac{\mathrm{R_{min}}(1 - D_{\mathrm{min}})^2}{2D_{min} * f_{min}} \tag{1}$$

$$L_2 \geq \frac{R_{max}(1 - D_{\mathrm{min}})}{2f_{min}} \tag{2}$$

$$C_1 \geq \frac{D_{max}}{R_{min} * f_{min} * \Delta V_{C1}} \tag{3}$$

$$C_2 \geq \frac{1 - D_{min}}{8 * \Delta V_{C2} * L_2 * {f_{min}}^2} \tag{4}$$

The results of these equations can be seen in Table X. Note that the values in the table are minimum values.

Table X. Component Values

Parameter	***Value***
L_1	120 µH
L_2	38 µH
C_1	26 µF
C_2	2.5 µF

LTSPICE simulations were then used to determine if the calculated values gave the desired function of the circuit. This was done by modeling the circuit in LTSPICE then using the STEP command to vary the duty cycle of the MOSFET from 20% (teal) to 70% (grey). The plots of the DC-DC convert output for the varying duty cycles can be seen in Fig. 2. A table of the ideal output for each duty cycle can be seen in Table XI. These values were calculated using equation (5) which is the ideal relationship between input and output for a Ćuk converter. By comparing the values from Fig. 2 and Table XI, it can be seen that the circuit functions as expected. The small discrepancies between the ideal output and the simulated output are due to non-ideal switches, including the voltage drop across the diode.

$$V_o = V_s\left(\frac{D}{1-D}\right) \tag{5}$$

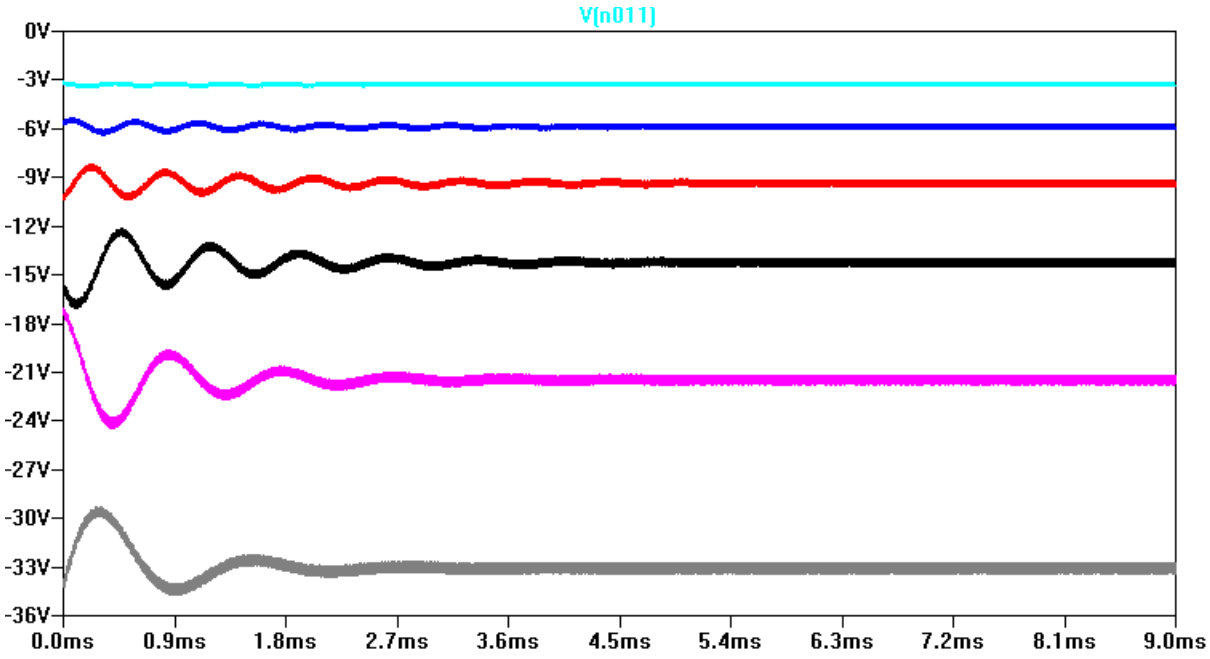

Fig. 2. LTSPICE Simulation of Ćuk Converter with Varying Duty Cycles

Table XI. Ideal Outputs

Duty Cycle	Ideal Output	Color
20%	-3.75	Teal
30%	-6.42857143	Blue
40%	-10	Red
50%	-15	Black
60%	-22.5	Pink
70%	-35	Grey

After it was determined that the circuit functioned as designed, maximum current and voltage rating for each component were determined from the LTSPICE model. These max specifications can be seen in Table XII.

Table XII. Maximum Specifications for Components

Component	Max Voltage (V)	Max Current (A)
L1	16	8
L2	21	3
D	20	10
C1	20	9
C2	20	~0.5
M1	27	10

Using the minimum values from Table X and the specifications from Table XII components were selected from www.digikey.com. Values and specifications of the selected components can be seen in Table XIII.

Table XIII. Selected Components

Component	Value	Max Voltage (V)	Max Current (A)
L1	120 uH	-	9.9
L2	56 uH	-	10.2
D	-	60	10
C1	27 uF	63	-
C2	3.3 uF	25	-
M1		75	100

In addition to the DC-DC converter. Voltage and current sensor were also needed for this design. It was determined that using the ADC built in to the MSP430 offered the easiest and lowest cost solution for voltage and current sensing. A reference voltage of 1.5 V was selected for the ADC. In order the scale the input voltage from a range of 0 to 38 V to a range of 0 to 1.5 V, a voltage divider was used. A diagram of this resistive divider topology can be seen in Fig. *3*.

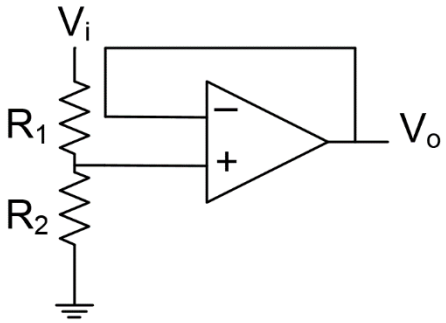

Fig. 3. Voltage Divider with Op-Amp Buffer

It was determined that a voltage of 64 V should correspond to 1.5 V on the voltage divider. An input/output ratio of 0.0234 was thus determined for the voltage divider. Using equation (6), values of R_1 = 470 kΩ and R_2 = 11 kΩ were selected from available resistors. This corresponded to an input/output ratio of 0.029. Large resistors were selected for this application in order to limit current through the voltage divider. An OP-AMP was used to buffer the output of the voltage divider before passing the signal to the ADC for reading.

$$\frac{V_o}{V_i} = \frac{R_2}{R_1+R_2} \tag{6}$$

For the output voltage sensor the voltage needed to be inverted as well as scaled since the output of a Ćuk converter is negative. This was accomplished using an OP-AMP inverting amplifier configuration. This configuration can be seen in Fig. 4. Equation (7) can be used to find the input/output relationship for the inverting amplifier. For ease of programming, it was determined that it was best to keep the same ratio for both input and output voltage sensors. Thus using (7) the values of R_1 and R_2 were determined to be R_1 = 47 kΩ and R_2 = 1.1 kΩ. Lower values were selected for R_3 and R_4 versus R_1 and R_2 since these resistors did not provide a path to ground, and thus excess current traveling through them was not a concern.

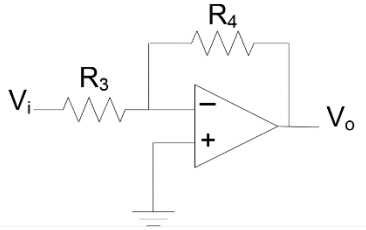

Fig. 4. Inverting Amplifier Configuration

$$\frac{V_o}{V_i} = -\frac{R_4}{R_3} \tag{7}$$

A shunt resistor was determined to be the easiest way to measure current in the design. A shunt resistor is a small resistor which is placed in series with the load. The current traveling through the load is proportional to the current flowing through the load. A 5 mΩ shunt

resistor was chosen. However, even at max rated current of 10 A, the voltage across this 5 mΩ resistor would be only 50 mV. In order to amplify this signal a current shunt monitor was used. This current shunt monitor amplified the voltage across the resistor with a gain of 20, thus putting the signal within a range which could be read by the ADC. A diagram of this current sensing topology can be seen in Fig. 5.

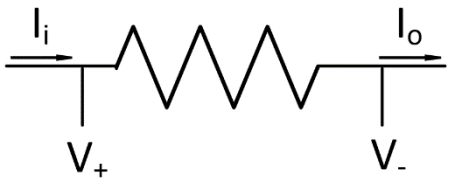

Fig. 5. Current Shunt Resistor Configuration

The Ćuk Converter and sensor circuits were then integrated into a final circuit. A diagram of this circuit can be seen in Fig. 6.

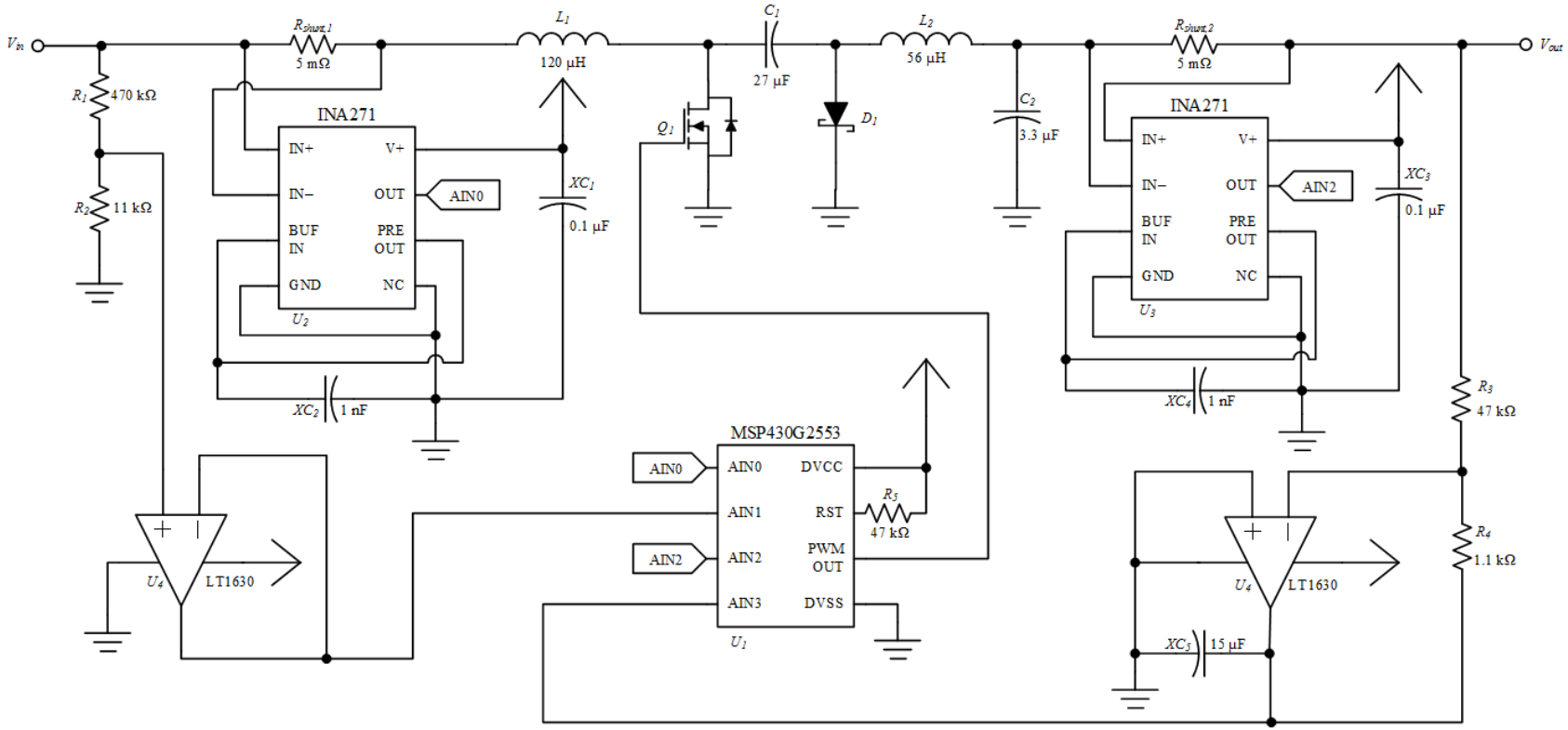

Fig. 6. Ćuk Converter with Integrated Sensors

In order to power the MSP430 as well as the op-amps and current shunt monitors a linear regulator was chosen. This linear regulator lowers the input voltage to a constant 3.6 V. This voltage was chosen as it is high enough to fully saturate the logic level MOSFET used in this design, which is important for using the MOSFET as a switch. Because a 3.6V regulator was not available, a variable output regulator was purchased. The voltage output of this regulator was determined based on two external resistors using the configuration in Fig. 7 and equation (8). By setting V_{out} equal to 3.6 and solving for R_2/R_1 it was found that that ratio of R_2 to R_1 should be approximately 1.88. Using resistor values which were then chosen from available resistors. R_1 was selected to be 2 kΩ and R_2 was selected to be 3.8 kΩ.

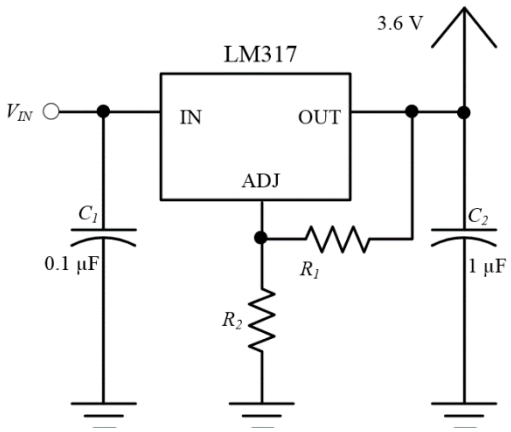

Fig. 7. Linear Regulator Configuration

$$V_{out} = 1.25(1 + \frac{R_2}{R_1}) \quad (8)$$

A printed circuit board was then designed for the circuit. The required trace widths were first calculated using an online tool [2]. Two net classes were defined. The first was a power class which could handle up to 10 A of current. It was determined that having these power traces on both the top and bottom of the board would best allow for this large amount of current which minimizing the needed trace width. The second net class was a data class which did not need to handle high currents, but instead moved signals across the board. Each of the components selected from Digi-key were modeled in Eagle then used to create a schematic and then board layout. For the board layout the *autorouter* function was first used to begin routing traces. Traces which could not be completed by the *autorouter* were then completed by hand. The final PCB layout can be seen in Fig. 8.

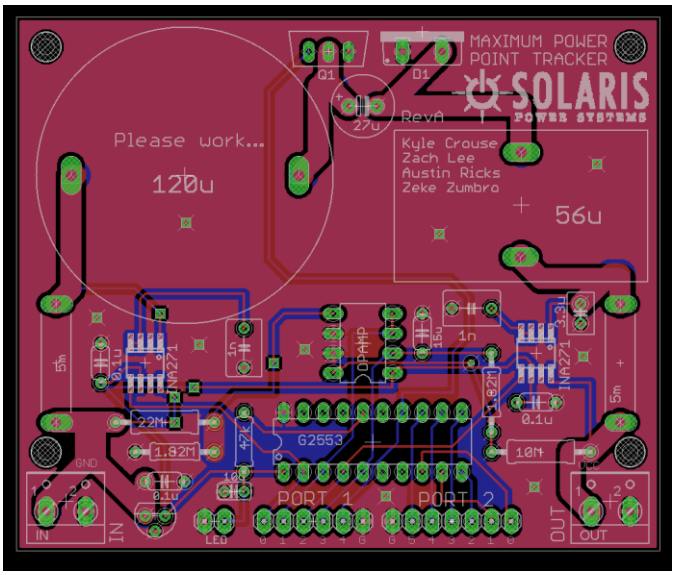

Fig. 8. Printed Circuit Board Layout

In addition to the electrical hardware components of this design, the software which runs on the MSP430G253 is extremely important. It is this software to enables the design to track the maximum power point, and provides the DC-DC converter with the switching signal that it needs to function. The code for this design can be seen in Appendix A. The code can be roughly divided into three sections; initialization, sensor reading, and maximum power point tracking.

The first of these divisions, initialization, contains the code which sets up the microcontroller and required peripherals. This initialization includes the functions Setup_MSP, Setup_ADC, Setup_PWM, and Setup_Timer. The initialization of each peripheral was divided into separate functions to that it was clear where the settings for each was located. This allows for greater readability of code and will make maintaining this code easier in the future. The clock speed of the MSP430 was set to 16 MHz in order to allow for the maximum number of duty cycle steps when running pulse width modulation (PWM) at 100 kHz. The ADC was configured to read 4 channels 32 times consecutively. This allowed for sampling each of the 4 sensors as well as averaging over 32 samples in order to take more accurate readings. The number of samples was chosen to be 32 since 32 is a power of 2 and thus division by 32 can be accomplished using a bit-shift which is more efficient than a normal integer division. TimerA0 was configured for PWM, and set to a frequency of 100 kHz by setting TACCR0 to 160. This value was determined by dividing the clock frequency, 16 MHz, by the desired frequency 100 kHz. PWM was set up to output on P1.6.

The next division of code was reading from the sensors. This section consists the function Read_ADC and the interrupt service routine (ISR) for the ADC. When Read_ADC is called, the ADC enable conversion flag is first cleared. The function then waits if the ADC is currently busy. The data from the ADC is then directed into an array of unsigned integers,

and sampling and conversion is started. The processor is then placed into low power mode 3. When the ADC has finished sampling, the ADC ISR is called and the processor exits low power mode. After ADC measurements have been taken, the 32 samples from each sensor are first added together, then this value is divided by 32 to find the average. This average is then put through a linear equation to relate the ADC value for each sensor to its actual measurement (volts or amps). This equations were determined using linear regression from data taken during testing. In order to get this data, known voltages were fed into the input of the circuit. The current in, as well as the voltage and current out were then measured using digital millimeters. At the same time the ADC measurements taken from the sensors on the board were also read. The data from this experiment can be seen in Table XIV. The linear regression tools from Microsoft Excel were then used to find equations relating voltage or current to the corresponding ADC value. The equations relating ADC reading and actual measurements can be seen in equations (9) through (12).

Table XIV. ADC Calibration Data

Input				**Output**			
Current (A)	Current ADC	Voltage (V)	Voltage ADC	Current (A)	Current ADC	Voltage (V)	Voltage ADC
0	3	0	11	0	12	0	8
0.043	7	0.5	11	0.046	12	0.101	6
0.157	12	1	18	0.17	10	0.37	7
0.296	23	1.5	25	0.307	15	0.667	8
0.46	32	2	32	0.457	29	0.994	14
0.646	42	2.5	41	0.628	41	1.36	20
0.84	55	3	48	0.8	55	1.74	28
1.06	75	3.5	57	0.999	72	2.16	35
1.28	91	4	66	1.18	88	2.57	42
1.53	111	4.5	71	1.39	104	3	49
1.84	136	5	78	1.62	124	3.5	58
2.18	163	5.5	91	1.88	145	4.05	68
2.54	191	6	95	2.12	165	4.6	77

$$I_{in} = 0.013459 I_{in_{ADC}} + 0.01594 \quad (9)$$

$$V_{in} = 0.066097 V_{in_{ADC}} - 0.27437 \quad (10)$$

$$I_{out} = 0.013002 I_{out_{ADC}} + 0.019945 \quad (11)$$

$$V_{out} = 0.061412 V_{out_{ADC}} - 0.05239 \quad (12)$$

The final division of the program for this design was the actual maximum power point tracking function. Many MPPT functions were developed, however the one chosen for this

design utilized the simplest MPPT algorithm, Perturb and Observe. A flow chart of the Perturb and Observe algorithm which was provided by Microchip can be seen in Fig. 9 [1]. In the Perturb and Observe algorithm the MPPT can be in one of two states, incrementing or decrementing. If the MPPT is in the incrementing state, then the duty cycle was last increase, if it is in the decrementing state, then the duty cycle was last decreased. In order to determine if the duty cycle would be incremented or decremented, the current instantaneous power was compared to the previous instantaneous power, if the power increased, then the state would remain the same and the duty cycle would be incremented or decremented based on its state. If the power instead decreased then the state was toggled, and the duty cycle would be incremented or decremented accordingly.

In order to make sure that the duty cycle never left its allowable range, if statements were used to make sure that the duty cycle was never incremented beyond its max duty cycle or decremented beyond it minimum duty cycle. These maximum and minimum duty cycles were set at 80% and 20% respectively. If the duty cycle was supposed to be incremented, but was already at its maximum value the duty cycle was instead decremented and the state was changed to decrement. The opposite was done if the duty cycle was supposed to be decremented but was already at its minimum value. This ensured that the MPPT would never get stuck at its maximum or minimum duty cycle.

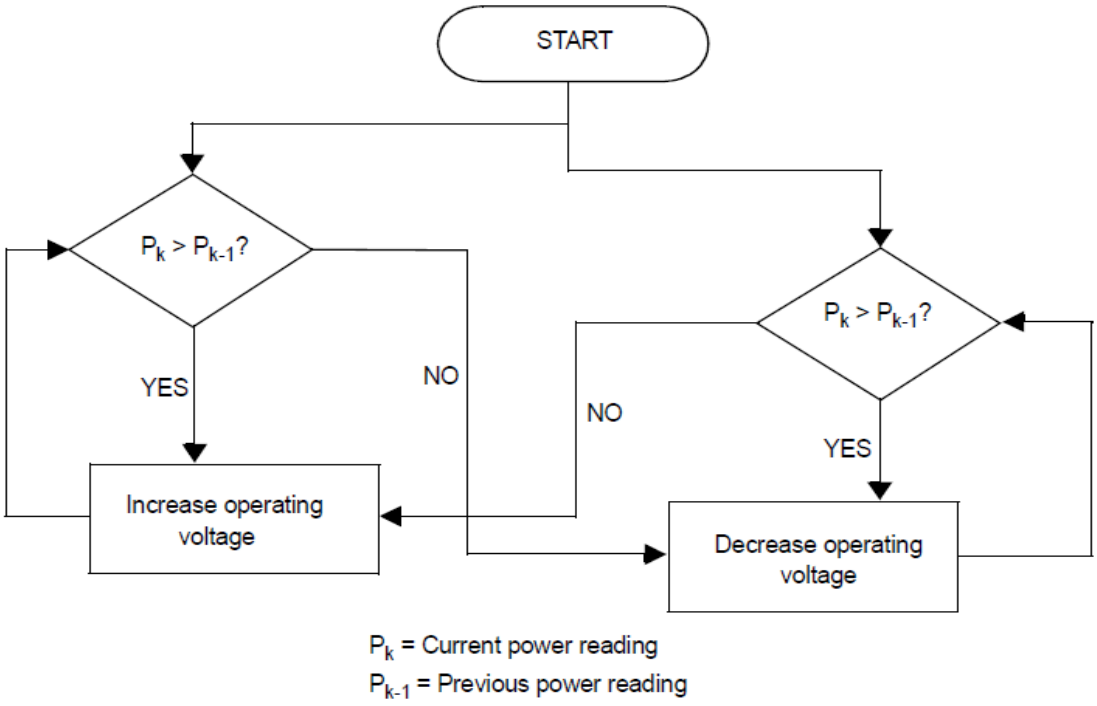

Fig. 9. Flow Chart of Perturb and Observe Algorithm [1]

2. Mechanical Details

The mechanical aspect of the MPPT began with the following requirements: weatherproofing including water resistance and the ability to withstand high temperatures, protection for the circuit against small impact and rough transportation, and adequate heat dissipation from the circuit to the outside air. A couple of ideas for housing material included printed ABS, purchased injection molding plastic enclosures, purchased extruded aluminum enclosures with outward facing fins, aluminum sheet metal, and purchased ammunition boxes. The choice was made to purchase a NEMA 4 die-cast aluminum enclosure. NEMA 4 is a rating from the National Electrical Manufacturers Association that ensures protection to the user from hazardous part, protection to the enclosure interior from dust, dirt, water, and ice formation. This rating completely fulfills most of the housing design requirements. The purchased enclosure offers the following benefits to the product design:

- The die-cast aluminum is an excellent heat conductor and will dissipate heat from the circuit directly to the outside air.
- The removable lid allows the user access to the circuit for installation and maintenance.
- Mounting holes are available at opposite corners of the box to allow the enclosure to be screwed directly onto a surface.
- A silicon gasket is used that will firmly and durably seal the enclosure with the lid on and tightened.
- Board mounting holes are available inside the box to securely attach a PCB directly to the enclosure.

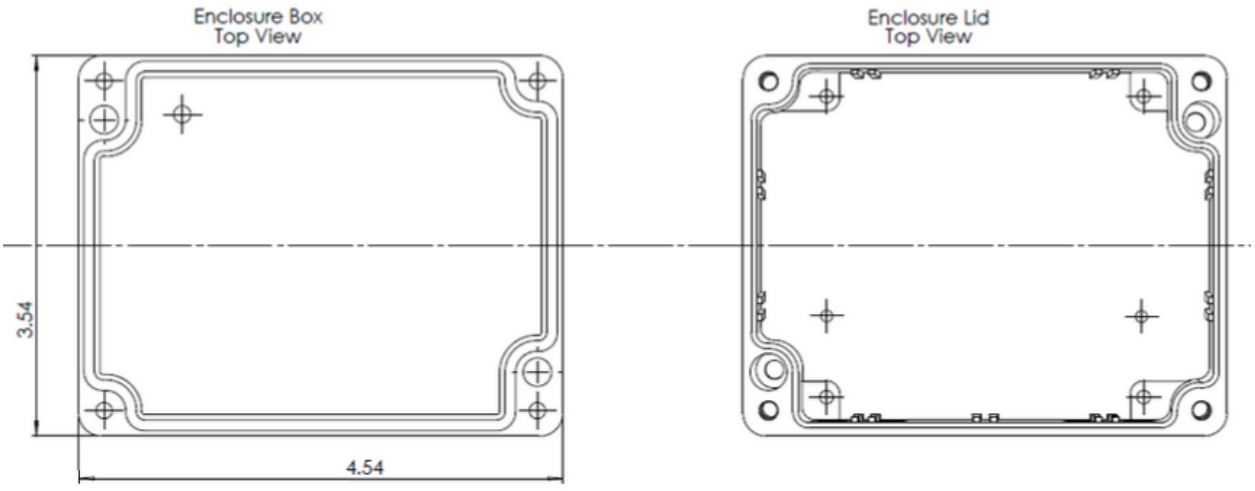

Fig. 10. Top View of Enclosure Box and Lid Draft and Dimensions

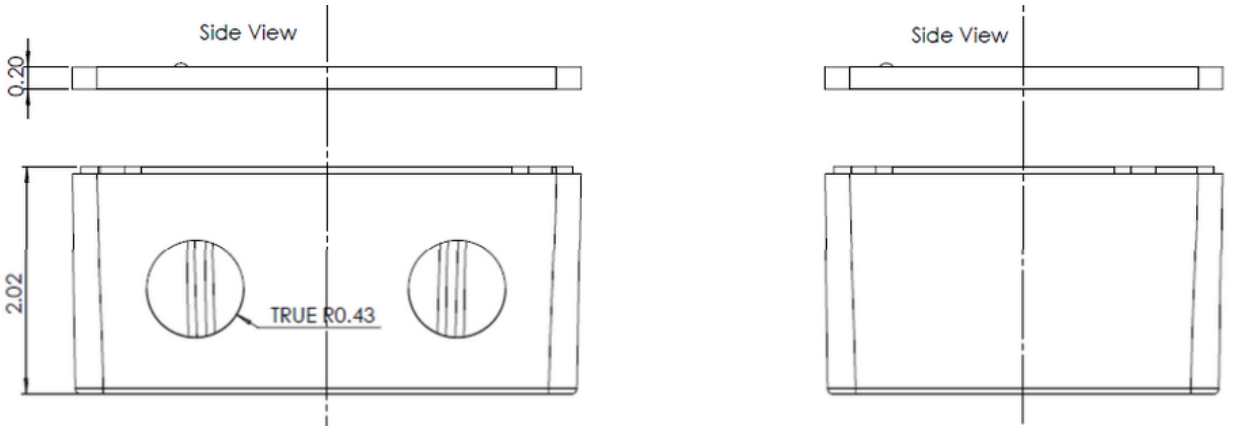

Fig. 11. Side Views of Enclosure Box and Lid Draft and Dimensions

Drawings and general dimensions for the box and lid are included below in Fig. 10 and Fig. 11.

As shown in Fig. 10 and Fig. 11, additional holes were drilled in the enclosure to fit product needs. Two large holes with a 0.86in diameter were drilled on the side of the box for the use of cable glands. Two small holes were drilled in the bottom of the box for screws to come up and screw into PCB standoffs, securing the PCB to the enclosure. Finally, a small hole was drilled in the lid for an LED circuit function indicator. The PCB is mounted inside of the box with one side screwed into the mounting holes in the box itself. When the enclosure was ordered, there was no expectation of using the mounting platform provided. However, one side of the PCB mounting holes line up almost perfectly with those of the box. A dremel sanding bit was used to widen the holes slightly and then M3.5 x 6mm screws could be used to attach at least half of the PCB to the box. The PCB was not as wide as the enclosure was and did not reach the mounting holes on the other side. Therefore, double side standoffs were used. Initially, aluminum standoffs were used until it was discovered that the PCB mounting holes are very close to the soldering connections for the current sensors and the aluminum would make electrical contact with the circuit. So plastic insulated standoffs were purchased. Screws were used to attach the PCB to the upper half of the standoffs, and then holes were drilled into the bottom of the box as stated earlier and screws came up from the outside of the box into the bottom half of the standoffs. This mounted the PCB at four corners to the enclosure box. Drafts of the standoff and bottom screws are shown below in Fig. 12. Also shown is the heat spreader. This heat spreader was created from a simple 6ft long rolled piece of aluminum purchased at the local hardware store. A small section was cut off and ground flat and smooth to act as a heat spreader between the MOSFET and diode heat sink surfaces and the enclosure box wall. The gap between the heat sink surfaces was large enough that two heat spreaders were required face to face. Thermal grease was used between every face to face contact to minimize air gaps and maximize surface to surface contact and thus heat dissipation.

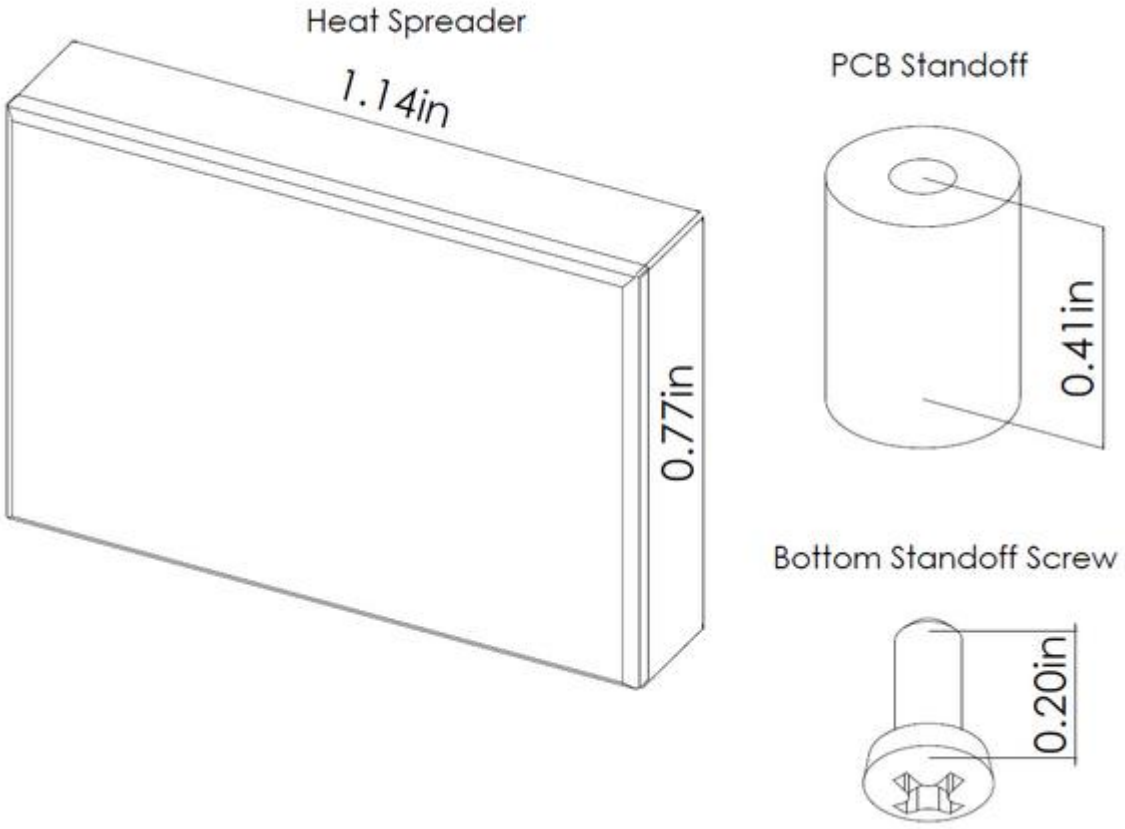

Fig. 12. Heat Spreader, PCB Standoff Screw Draft and Dimensions

Input and output cabling between the panel, circuit, and load provided the challenge of figuring out how to make weatherproof and strain relieving cable connections. Cable glands were the solution for both of these requirements. The cable enters the gland body, the rubber washer is placed on the cable gland and butted up against the outside of the enclosure, the lock nut is placed on the gland body thread inside of the box and tightened up against the box wall, and the nut is tightened. Tightening the gland nut clamps a piece of plastic and rubber onto the cable. The plastic grabs the cable for strain relief and the rubber forms a waterproof seal around the cable. The minimum cable size allowed by the cable glands purchased is 0.2in in diameter. This pertains to a 4 AWG cable, not considering insulation. The cable used for testing was 0.21 inches in diameter and sheathed three 20 AWG cables. Drafts for the cable gland components are shown below in Fig. 13 and a rendering is shown in Fig. 14.

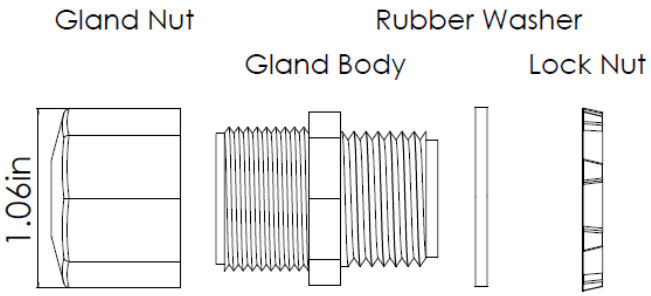

Fig. 13. Cable Gland Components Side View, w/o Plastic/Rubber Clamp Bit

Fig. 14. Cable Gland Assembly

The printed circuit board and select circuit components were modeled in SolidWorks for use in a final product assembly. This PCB assembly is shown below in Fig. 15. It will be used in final models to indicate the use of heat spreaders, standoffs, and proximity to enclosure walls and cable glands. The MOSFET and diode were chosen to be modeled because they played a crucial role in heat dissipation. The inductors were modeled to indicate the height of the circuit. Finally, the pins were modeled because they were simple to make.

A final assembly is shown below in Fig. 16 and Fig. 17.

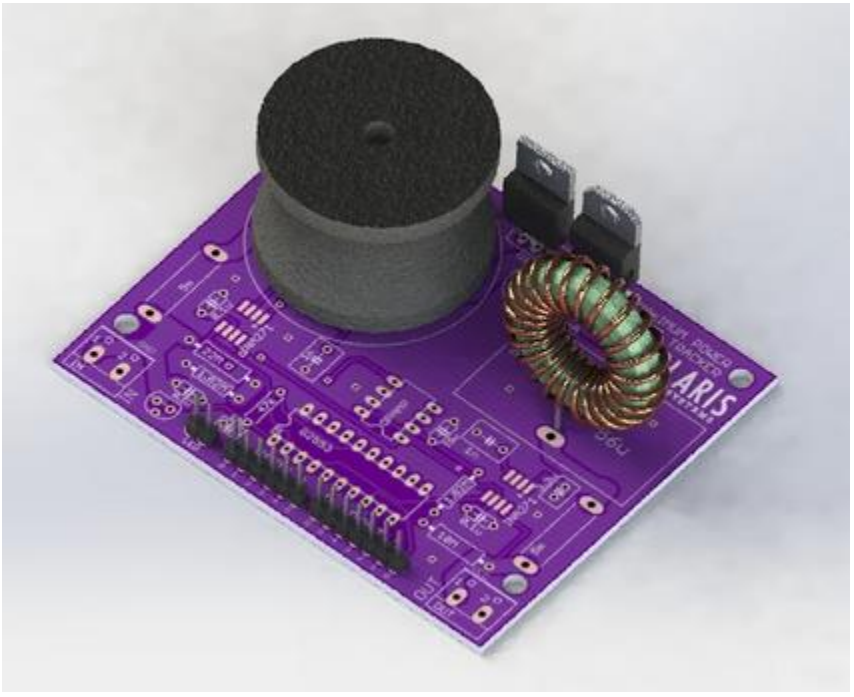

Fig. 15. PCB Assembly with Select Components

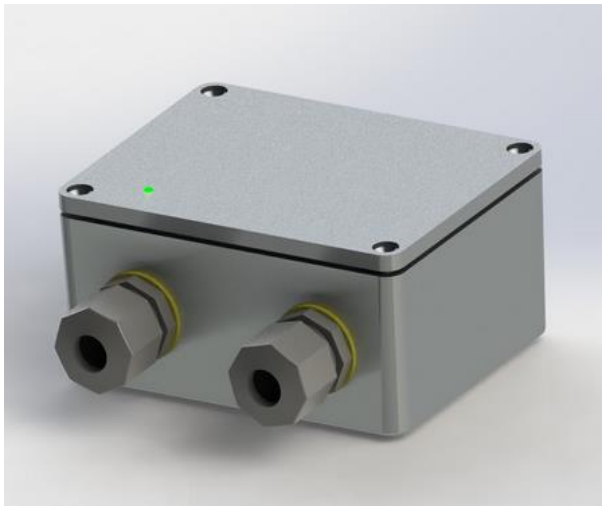

Fig. 16. Final Product Assembly with Lid

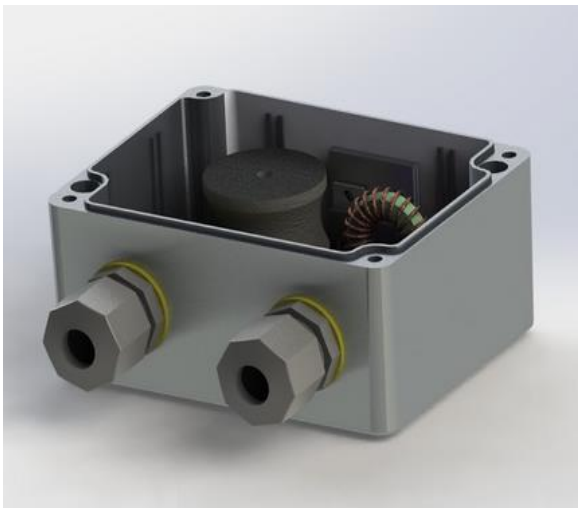

Fig. 17. Final Product Assembly without Lid

D. Reliability & Safety (FMECA)

The FMECA has been divided into seven major items, which account for the major subsystems of the device. For each item, the failure modes were determined, followed by the failure causes, and failure effects. Given these three attributes, a severity index of value 1 to 4 was assigned, 1 being insignificant, 2 being marginal, 3 being critical, and 4 being catastrophic. A probability index of value 1 to 4 was assigned, 1 being extremely remote, 2 being remote, 3 being reasonably probable, and 4 being probable. A third index, criticality, was determined by multiplying the severity and probability indices to give further guidance for ranking potential failures. Given these rankings, control measures were determined to limit the possible failure modes.

i. Current Sensors

Shunt resistors can fail due to a flow of current greater than the specified rating. However, since the resistors have such a low resistance, they are rated for extremely high amounts of current, thus the only likelihood of them failing is due to a physical flaw within the resistor. A physical flaw would cause the resistor to fail, producing an open circuit, thus separating the input from the DC-DC converter. This is not harmful to the PV panel or the DC-DC converter, however, it does result in a non-functioning device, thus a severity of 2 has been assigned. A shunt resistor can also fail by a short circuit due to improper placement or soldering, which causes the microprocessor to be unable to measure the current flowing into the converter. This then affects the power point since it can no longer be tracked by the processor, resulting in an improperly functioning device with unpredictable results. Given these considerations, a severity of 3 and a probability of 1 has been assigned. The most practical way to limit either of these failure modes is to ensure the use of quality sensors.

ii. Voltage Sensors

The voltage sensor is created by two large resistors functioning as a voltage divider, which the analog-to-digital converter can then use to sense the voltage. These resistors can fail open if too much power is supplied to the resistors, causing them to burn out. This would hinder the microprocessor from sensing the voltage, resulting in an improperly functioning device with unpredictable results, thus a severity of 3 and a probability of 1 has been assigned. These resistors can also fail by creating a short circuit to ground, caused by an applied voltage higher than the rating. This would then short the entire panel to ground. This does not harm the panel, however, it does result in a non-functioning device, and thus a severity of 2 and a probability of 1 has been assigned. The most practical way to limit either of these failure modes is to ensure the use of quality sensors.

iii. DC-DC Converter

While the DC-DC converter contains numerous components, the MOSFET and diode were concluded to be the most vital when considering failure.

The MOSFET has two failure modes: open circuit and short circuit. An open failure can be caused by overcurrent or overvoltage from the photovoltaic array and results in no output voltage. A lack of output voltage damages no components or equipment, but results in a non-functioning device, thus a 2 was chosen for severity. A probability of 2 was chosen, as this failure mode is remotely likely to happen given consistent use over a span of time. A closed circuit failure of the MOSFET can be caused by overcurrent and results in the input source being shorted. Shorting a photovoltaic panel results in no damage to the panel, but does result in a non-functioning device, thus a 2 was chosen for severity. A probability of 2 was chosen, as this failure mode is remotely likely to happen given consistent use over a span of time. These failure modes can most practically be limited by ensuring appropriate safety factors in current and voltage for the MOSFET.

The diode also has failure modes of open circuit and short circuit. A short circuit is caused by overvoltage when the diode is in reverse bias. A short across the diode results in no output voltage. A lack of output voltage damages no components or equipment, but results in a non-functioning device, thus a 2 was chosen for severity. A probability of 2 was chosen, as this failure mode is remotely likely to happen given consistent use over a span of time. An open circuit failure of the diode is caused by continual overvoltage after the diode has reached a short circuit failure. An open across the diode results in no output voltage as well as overvoltage across the other components. This would likely damage the components, leading to a more severe failure. Additionally, this results in a non-functioning device, thus a 4 severity. A probability of 2 was chosen, as this failure mode is remotely likely to happen given

consistent use over a span of time. These failure modes can most practically be limited by ensuring the use of a quality diode.

iv. Microprocessor

The microprocessor is the brain of the maximum power point tracker. It runs the software which reads inputs from the current and voltage sensors and uses this to adjust the duty cycle of the switched mode DC-DC converter.

The microprocessor can fail in two ways. The first of these failure modes is lack of power. Three possible causes for lack of power to the microcontroller have been identified. The first of these is that there is an alternative path to ground which is diverting current from the microcontroller and preventing the microcontroller from receiving the necessary voltage. This could be caused by any component failure which shorts the input source, such as a short circuit of the input voltage sense resistor, or a short of the MOSFET. Alternatively, lack of power to the microcontroller could be caused by not having a PV panel attached to the MPPT or voltage input from the panel being below the cutoff of the microcontroller regulator. As there are many causes for this failure mode, a probability of 3 was assigned to this failure mode, signaling that it is fairly likely to happen. However, the severity of failure is a 1, as in most cases lack of power to the microcontroller only happens when the MPPT should not be functioning anyway, and the microcontroller will not be damaged by lack of power. Finally, lack of power to the microcontroller could be caused by failure of the linear voltage regulator. In order to avoid this, a reliable linear regulator will be chosen, also the probability of failure modes which will cause a short of the input panel will be minimized.

A second failure mode for the microcontroller is power overload. This can result from failure of the linear regulator. The severity of this failure is a 3, since power overload will damage the microcontroller, and possibly destroy it. However, since linear regulators are designed to fail in such a way as to protect the loads they are attached to, this failure mode is very unlikely to occur, so it was given a 1 for probability. This failure mode will be controller by selecting a reliable voltage regulator.

v. Software

The software for this project is as important as the microcontroller which runs it. Three possible failure modes of the software were identified. The first of these failure modes was variable overflow errors. These errors can occur whenever something is added or subtracted from a variable so that it overflows it allotted number of bits. This can cause errors in software such that variables cannot be accurately read, which can affect the ability of the software to identify the maximum power point. With proper software design, it is unlikely that these errors will occur so a probability of 1 was assigned to this failure mode. If this error does occur, the system may not be able to

find the MPP, however lasting damage will not be done, as resetting the microcontroller should solve the problem, thus a severity of 1 was assigned to this failure mode.

A second failure mode of the software will be failure to find the MPP. The primary cause of this type of error will be false peaks as the software searches for the MPP. This is fairly likely to occur as transients from changing the switching duty cycle and changes in weather conditions can cause false peaks in the power calculation, so a probability of 3 was assigned to this failure mode. This is not a very serious failure however, as the software is constantly searching for the MPP and is likely to eventually find the MPP even if false peaks occur. Also, this failure does not cause any permanent damage, and thus is less severe. A severity score of 1 was assigned to the failure to find MPP failure mode. Failure to find the MPP will be mitigated by using a software filter to smooth the power waveform in order to minimize false peaks.

A final failure mode of the software component of this design is a timing error. These errors can occur when interrupts are not properly prioritized or interrupt service routines are too long. This will affect the ability of the circuit to find the MPP and its ability to correctly set the duty cycle of DC-DC converter. These timing errors are fairly likely to occur, as interrupts are somewhat difficult to predict. However, these timing errors do not cause permanent damage and are unlikely to significantly affect the operation of the MPPT, thus a severity score of 1 was given to this failure mode. In order to prevent timing errors, interrupt service routines will be kept as short as possible, and critical interrupts will be given highest precedence. In addition, interrupts will be disabled when time critical code is running.

vi. Housing & Connectors

Housing failure can be detrimental to product function. If water or dirt are able to get inside of the housing, the electrical circuit can be severely damaged. Since water is electrically conductive, it is able to significantly affect circuit function. Components can be damaged beyond repair through short circuiting. Failure to protect the circuit can come from housing failure and connector failure. The housing can be built poorly and provide inadequate sealant, can deform from temperature changes coming from both the weather outside and the circuit inside, and can be dropped and mishandled in a way that causes cracks and loses its seal. The connector, connecting the leads from the solar array and the leads that run to the load and/or battery, can open up the circuit to the outside through the inability to seal with varying sizes of leads and improper assembly. For example, though the connector design is not finalized, the preferred design will use a plastic cap that will screw onto a base with a rubber O-ring that clamps onto the wires. If the cap is not screwed on tight enough or the O-ring is broken or missing the connector will fail to seal. The severity of failure to seal

was assigned a 3 as the product will fail with enough water contacting the circuit and the user can be shocked if he/she comes into contact with water in contact with the circuit. The probability of failure at this level is low and has placed at a level 1. The housing and connector will be designed with weather resistance as a priority and the probability that they will lose that resistance over time is not high. Extensive testing will be done to ensure adequate resistance.

The housing can also inadequately dissipate heat from the interior. The sun and the circuit will both provide heat to the product, and the housing will need to be provide enough surface area contact with the environment to transfer enough heat to maintain circuit efficiency. This places importance on the material choice and shape of the housing.

The connectors can also fail in not providing enough grip on the cables to keep them connected to the circuit. The leads will experience certain levels of tension and the connectors will have to withstand these forces to keep contact and maintain a seal.

A summary of the FMECA can be seen in Table XV below.

Table XV. FMECA Summary

Item		Failure Mode	Failure Causes	Failure Effects	Severity	Probability	Criticality	Control Measures
Current Sensors		Open Circuit	• Overcurrent • Overvoltage	Short input source	2	1	2	Utilize quality Sensors
		Short Circuit	• Overcurrent • Overvoltage	Microprocessor unable to monitor current	3	1	3	
Voltage Sensors		Open Circuit	• Overcurrent • Overvoltage	Microprocessor unable to monitor voltage	3	1	3	Utilize quality Sensors
		Short Circuit	Overvoltage	Short input source	2	1	2	
DC-DC converter	*MOSFET*	Open Circuit	• Overcurrent • Overvoltage	No output voltage	2	2	4	Ensure MOSFET safety factors for both current and voltage
		Short Circuit	Overcurrent	Short input source	2	2	4	
	Diode	Open Circuit	Overvoltage	• No output voltage • Overvoltage on other components	4	2	8	Utilize high quality diode
		Short Circuit	Overvoltage	No output voltage	2	2	4	
Microprocessor		No Power	• Alternate path to ground • No panel connected • Voltage input below cut-off • Failure of voltage regulator	Nonfunctional circuit	1	3	3	• Prevent conditions which short the input • Choosing a reliable voltage regulator
		Power Overload	Linear regulator failure	DC-DC circuit failure	3	1	3	Appropriate safety factor
Software		Variable Overflow Error	Variables such as characters or integers are incremented above their range and overflow	• Software unable to correctly read variables • Could cause converter to create over- or under-voltage conditions.	1	1	1	Carefully choose variable types and operations to ensure that overflow conditions are avoided

	Failure to Find Maximum Power Point	False peak causes software to choose wrong maximum power point	Less than maximum power extracted from panel	1	3	3	Utilize smoothing filters to ensure that the software does not latch on to small peaks
	Timing Error	Improper precedence causes timing issues with interrupts	Less than maximum power extracted from panel	1	2	2	Correctly set precedences for interrupts and keep interrupt service routines short
Housing	Failure to seal interior from weather	• Deformation from heat • Mishandling of product • Faulty manufacture	• Circuit failure • Components are damaged • Possible shock of user	3	1	3	• Use adequate thermal conductivity in material choice • Exhaustively test for weather resistance
	Failure to adequately cool interior	• Inadequate Material • Inadequate Design	• Circuit efficiency depletes • Possible burn of user	2	3	6	
Connectors	Failure to seal interior from weather	• Connection not assembled correctly • Inadequate design for varying lead sizes	• Circuit failure • Components damaged • Possible shock of user	3	1	3	• Design to be flexible and accommodate varying lead sizes • Design to provide a tight hold on all cables
	Failure to maintain cable connection	• High tension on trailing leads • Inadequate hold on cables	• Leads are disconnected from product • No output voltage	1	3	3	

E. Prototype Construction & Integration

The process of building this design began with computer models. LTSPICE simulations and SOLIDWORKS models were completed to ensure that the design would function once built. This prevented many problems which could have occurred during the build process. A printed circuit board (PCB) was designed in EAGLE. After the board design was finished the dimensions of the board were used to plan the housing design for the MPPT. Since JBU does not have the capability of printing custom PCBs an outside company was used to manufacture this PCB. While this board was being printed, the components for the board were ordered. Once the PCB and all components for the design had been received, the circuit was assembled by soldering on each component. Surface mount components were soldered first, using solder paste and a heat gun. The through-hole components were then soldered in from shortest to tallest. Upon assembly, the initial idea was to test the circuit to hope that we finished by connecting it to a 65 W panel. This open-circuit voltage of this panel, 92 V, was too high for the linear regulator and caused it to fail, and provide over-voltage to many of the components on the board. When troubleshooting which components had failed, it was noticed that the operational amplifier was not functioning properly. Upon inspection it was found that the EAGLE model of the OP-AMP had the pins labeled in an improper order. In order to correct this a small solderable breadboard called a stamp was created to properly connect the operational amplifier to the circuit. During this analysis it was also brought to light that the resistors used in the original design were too large and caused the OP-AMP to not behave as an ideal OP-AMP. This problem was solved by reducing the resistance of the resistors in our OP-AMP circuit to kilohm range resistors instead of megohm range resistors.

While changing these resistors it was determined that the ADC reference voltage should be lowered, so new resistor values were selected to decrease the voltage which was fed into the ADC. The calculations to find these resistor value can be seen in the Technical Analysis section of this report. After making all these changes a new board was assembled since the IC chips on the first board were too difficult to replace. The second board was tested with a voltage source which could supply 44 Volts and 22 Amps. During testing a user error occurred where a voltage of 20 V with 7 A were applied to the circuit. This resulted in a 140 W being transferred through the circuit which exceeded the 100 W rating of the circuit. This caused the circuit to fail, although it was unclear what component or components had failed. Since the cause of this failure could not be determined, it was decide to repair the first circuit instead of continuing to debug the second. New current monitor chips were implemented to the first board. After verifying the current sensors were working, his circuit was tested and found to be functioning correctly. The next step was to make the board independent. This required finding a new linear regulator which could regulate the voltage properly to the standards needed for the MSP430G2553 to operate. A new variable output linear regulator was purchased. This regulator had a different pinout than the original regulator and also required two resistors in order to set its output voltage. A second stamp was designed to

integrate these resistors as well as connect the new linear regulator with the board. After verifying that this new linear regulator was functioning correctly. The whole circuit was tested.

Concurrently with the assembly of the circuit, a die-cast aluminum case was purchased to house the circuit. After this case was received two holes were drilled for the cable glands. These glands allow for wires to enter the housing while maintaining a water-tight seal. Two additional holes were drilled in the bottom of the case to allow for mounting screws for the PCB. A final hole was drilled in the top of the case for a small LED indicator light. After all holes had been drilled the case was tested for weather resistance. The interior of the case was then readied for the PCB by grinding down the interior ridges to make a smooth surface for the MOSFET and diode heat sinks to connect to. This smooth surface was important in order to insure maximum thermal conduction.

Once the housing components were ready, assembly began. The components include the enclosure box with holes drilled and one side smoothed, enclosure lid with LED hole drilled, LED soldered with a resistor and wires, two cable glands, PCB, PCB standoffs, two heat spreaders, thermal paste, and screws. The screws used are the four that attach the lid to the box, two that attach the PCB to the box, and two that attach the box to the standoffs. Assembly was done as so:

Thermal paste was applied to one heat spreader and placed firmly against the enclosure box wall. Thermal paste was applied to the second heat spreader and placed firmly against the first. The standoffs were then attached to the two mounting holes not in corners of the PCB. A notch had to be cut out of the plastic standoffs to accommodate current sensor soldering connections. The cables were then attached to the circuit terminals. This was done before placing the circuit into the housing because the circuit terminals were close enough to the cable glands to make attaching cables difficult. A note was made in the future product improvements section. The PCB was lowered into the housing and screwed into the enclosure box on the opposite side of the cable glands with the MOSFET and diode heat sinks facing the smoothed side of the enclosure wall. Screws were inserted into the holes in the bottom of the enclosure box and screwed into the bottom side of the standoffs. Thermal paste was applied to the MOSFET and diode heat sink faces and pressed firmly against the second heat spreader surface. The soldering connections for the MOSFET and diode caused them to pull away from the heat spreader surface at an angle, not allowing for a surface to surface connection. This was solved by adding a small dab of cyanoacrylate glue to the edges of the heat sinks, heat spreaders, and enclosure box wall. A small amount was used to allow for simple disassembly. The cable glands were tightened by holding the cables on the interior with pliers to prevent the cable from twisting as the nut is tightened which would pull on the connections to the circuit terminals. Finally, the LED wires were placed on the appropriate pins and the enclosure lid screwed down with the four corner screws. The LED wires were made to be long enough to not cause hassle when removing and placing the enclosure lid.

F. Testing & Verification

In order to verify that the design would function as designed, the individual subsystems of the design were first tested to ensure that they met specifications. The entire system was then tested to determine if it met the design goals.

The DC-DC converter subsystem was first tested to determine if it was able to vary the voltage output based on the duty cycle. An input of 5 V was applied to the DC-DC converter with duty cycles ranging from 25% to 62.5%. The results of this test can be seen in Table XVI. From the table, it can be seen that the output voltage did vary with the duty cycle as desired. The variation of the measured output voltage from its expected values from the ideal equation (5) and LTSPICE simulation can be attributed primarily to losses across the diode and MOSFET, as well as losses due to non-ideal components. This variation is not concerning in this design however, since the ideal equation will not be used to estimate the voltage output in this design.

Table XVI. Duty Cycle Testing Results

V_{in}	Duty Cycle	Ideal	LTSPICE	Measured
5.00	25%	-1.67	-1.38	-1.06
5.00	37.5%	-3.00	-2.62	-2.22
5.00	50%	-5.00	-4.53	3.91
5.00	62.5%	-8.33	-7.72	-6.83

The efficiency of the DC-DC converter was then tested. This testing by varying the duty cycle and input voltage of the DC-DC converter and measuring the input power and output power. The efficiency of the circuit was then calculated using equation (13). The results of this test can be seen in Table XVII. From Table XVII it can be seen that the average efficiency of the circuit was 74.61%. This exceeds the efficiency requirement of 70%. In subsequent designs efficiency will be increased. Methods to improve efficiency are discussed in the Future Work section of this report.

$$\eta = \frac{P_{out}}{P_{in}} \tag{13}$$

Table XVII. Efficiency Testing Data

Duty Cycle	Input Voltage (V)	Input Current (A)	Power In (W)	Output Voltage (V)	Power Out (W)	Efficiency
30%	5	0.13	0.65	1.65	0.45	69.46%
	10	0.29	2.9	3.57	2.11	72.88%
	12.5	0.39	4.875	4.65	3.59	73.56%
	15	0.49	7.35	5.72	5.43	73.82%
	17.5	0.58	10.15	6.78	7.62	75.11%

	20	0.71	14.2	7.95	10.48	73.81%
	25	0.96	24	10.4	17.94	74.74%
	30	1.32	39.6	13.4	29.78	75.20%
40%	5	0.32	1.6	2.66	1.17	73.34%
	10	0.74	7.4	5.83	5.64	76.17%
	15	1.2	18	9.12	13.79	76.63%
	20	1.77	35.4	12.85	27.38	77.35%
50%	5	0.71	3.55	4	2.65	74.74%
	10	1.75	17.5	9	13.43	76.76%
60%	5	1.65	8.25	6.11	6.19	75.04%
	6	2.07	12.42	7.5	9.33	75.11%

The sensors subsystem was then tested to insure that the current and voltage sensors could be used to accurately measure current and voltage in and out of the circuit. In order to do this testing, each sensor was evaluated by providing to it a known voltage or current using a DC voltage source and resistors. The output of the sensor was then compared to the reading from a DMM to determine if the output voltage of the sensor was linearly related to the input. The output of each sensor was then read using the MSP430 ADC. Linear regression was then used to relate the ADC values to the actual voltage and current values read by the DMMs. This test is discussed in further detail in the Technical Analysis section of this report. Table XIV. ADC Calibration Data contains the data from this test and equations (9) through (12) contain the resulting equations for I_{in}, V_{in}, I_{out}, and V_{out} respectively. Microsoft Excel was used to find the correlation between these equations and the measured values in Table XIV. All correlation coefficients were found to be greater than 0.993, meaning that these equations closely match the measured data.

The housing was first tested for weatherproofing by placing a piece of humidity sensitive paper inside the box then submerging the empty housing in water to a depth of 5 inches. The housing remained underwater for 5 minutes. The housing was then opened and the humidity sensitive paper was examined in order to determine if water had entered the housing. It was determined that no water entered the housing during this test. Since water was not able to enter the case when submerged, it was determined that the case was sufficiently weather proof.

After testing each of the subsystems, the final design was assembled. After assembling the full circuit the self-consumption of the microcontroller and sensors was measured by plugging the circuit into a 65W panel and measuring the current flowing out of the linear regulator using a DMM. Power consumed by the microprocessor and sensors was then calculated by multiplying this current by the voltage output of the linear regulator. The current output of the linear regulator was measured to be 17.5 mA and the voltage out of the regulator was

3.69 V. This yielded a self-consumption of 64 mW, which is 36 mW less than the 100 mW parameter set forth at the beginning of this design process.

The maximum power point tracking functionality of the prototype was then evaluated. This testing was done first using two 15 W Thunderbolt Magnum Solar PV panels located in the JBU Solar Lab. For this test with the MPPT outside its case and thus there was no heat sink for the diodes or MOSFET. The use of the 15 W panel for these tests ensured that the circuit would not be thermally damaged while the case was being completed. For this test, the MPPT with a 6Ω load resistor was connected to one 15 W PV panel while a 6Ω resistor was connected directly to another identical 15 W PV panel. Data for this test was taken using a digital oscilloscope which saved voltage readings every 0.2 seconds. The voltage across each resistor was measured so that power could be calculated using (14). This test was done for 450 seconds, which is the max time for which the oscilloscope can save data. The panels were then swapped and the test was repeated. It was determined from this data that both panels were not in fact identical and that one panel produce significantly more power than the other despite being the same model. This was found to skew the test data. However, since the testing was done on a cloudless day and both tests were run sequentially, it was determined that the MPPT data could be compared to the baseline data from the other trail so that both data sets would be from the same panel.

Data from these tests was then analyzed. From the instantaneous voltages, instantaneous power was calculated using equation (15). Excel was then used to calculate a 10 point moving average of the instantaneous power in order to smooth the instantaneous power curve. Plots of this smoothed instantaneous power curve can be seen in Fig. 18 and Fig. 19. From the figures it can be seen that the MPPT significantly increased the power delivered to the load resistor relative to the baseline test.

$$p(t) = \frac{v(t)^2}{R} \tag{14}$$

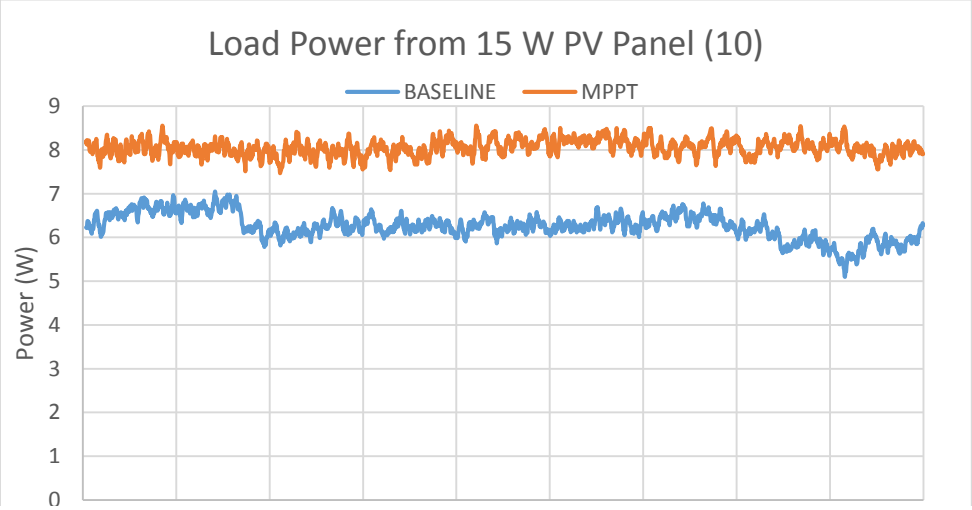

Fig. 18. MPPT Test for 15 W PV Panel at Station 10

The average power dissipated over the duration of the test was then calculated by first calculating the RMS voltage of each test using equation (15).

$$V_{RMS} = \sqrt{\frac{1}{N}\sum_{n=0}^{N} v(n)^2} \tag{15}$$

The RMS voltage was then used to find average power using (16). These average power values were then compared to determine the percent increase in power using the MPPT using (17). It was found that the percent increase in power for the 15 W panel at station 9 was 41.71% and the percent increase for the panel at station 10 was 28.77%. This gave an average percent increase of 35.24% which is well above the required percent increase of 10% for the design to be considered successful. It is important to note that this percent increase includes the lower than desired efficiency of the DC-DC converter. If this efficiency could be increased, the over percent increase of power would be increased as well.

$$P = \frac{{V_{RMS}}^2}{R} \tag{16}$$

$$\Delta P = \frac{P_{MPPT} - P_{BASE}}{P_{BASE}} \times 100\% \tag{17}$$

Temperature testing was conducted using the PCB circuit inside of the sealed housing. Two thermocouples were used to read temperature levels as the circuit was given 25 W of power with a roughly constant 2 A input. One thermocouple was placed above the heat spreaders for the MOSFET and diode and the other thermocouple was placed in ambient space above the middle of the circuit. Testing was done over the span of about 60 minutes until the temperature did not significantly change over time. Maximum temperatures of the individual circuit components were found from the data sheets. This indicated a maximum circuit temperature of 185°F. Testing results showed an equilibrium temperature of 120°F inside of the product, with outside ambient temperature at 77°F and a 25 W input.

From the tests run on this design it was determine that the circuit met the criteria set forth for it in most categories. Testing showed an average DC-DC converter efficiency of 75% which was 5% higher than the requirement of 70%. The average ΔP for the circuit was 35.24% which exceeded the ΔP requirement of 10% by 25.24%. In addition, self-consumption for the circuit was measured to be 64 mW, which us 36 mW less than the design requirement of 100 mW. Thermal testing showed max temperature of 120°F, which was 65°F less than the requirement of 185°F. Finally, while the initial design called for the circuit to handle up to 100W, the circuit was only tested with up to a 65W panel. While the component specifications should allow for 100W, the circuit can only be verified up to 65W.

IV. Schedule & Modifications

The schedule was originally broken down into four pieces: research, design/troubleshoot, assembly, and testing of the prototype; however this overlooked documentation, manuals, and other written portions of the design process. This documentation was added to the length of time required to complete task. Most of the schedule elements overlapped with another, however there were certain tasks such as programming and troubleshooting which depended on the completion of other tasks before they could be started. The completion of prior tasks such as troubleshooting for all the components led to delays that could only begin once the initial problem was solved. To begin the process of making an MPPT, the first step was to have time to research how an MPPT works, along with reading articles on DC-DC converters used in MPPT applications. This took a significant portion of time since there were other assignments for junior design during this research phase. The design portion included the printed circuit board (PCB) along with the housing of the MPPT. Some mistakes were made with components selection and PCB layout which led to a significant amount of time spent troubleshooting. There were not as many problems with the mechanical side of the MPPT. The housing components were not all gathered until late in the semester. Extensive planning was done for choosing which components to use, but acquiring them so late left little to no room for major revisions if major revisions became necessary. Thankfully, all the components functioned as expected and provided a waterproof enclosure interior that dissipated circuit heat at a reasonable rate. The original plan left more time for testing than was done. Extensive temperature testing would be ideal for a wide variety of input wattage. The assembly phase is where the final PCB and the mechanical housing come together to create the final MPPT. The testing phase is to show data for the final presentation and to verify that the prototype meets all the requirements. This was the final step after assembly. Overall the timeline did not change significantly over the course of the semester. Events were lengthened and shortened with respect to one another, but there was not too much added to the timeline. The timeline can be seen in Fig. 20 below.

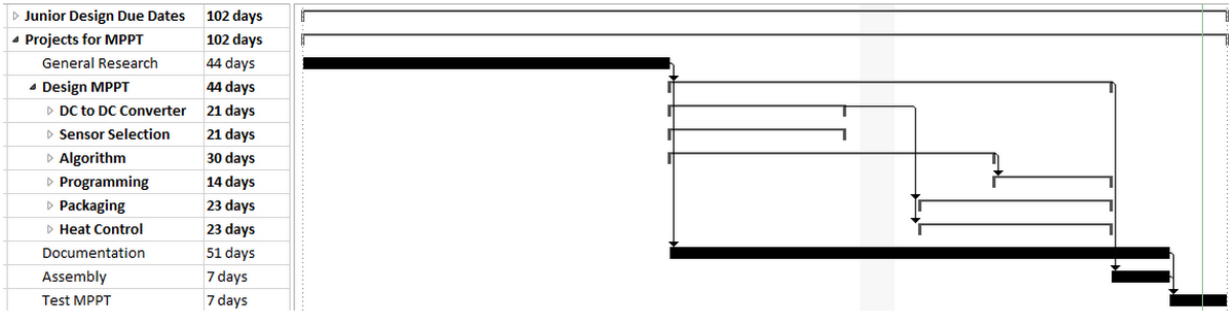

Fig. 20. Timeline

V. Final Budget & Future Production Costs

The final budget from the project can be seen in Table XVIII. As shown, we remained well within our budget, having an excess of approximately $550 upon project completion. The vast majority of expenses were in electrical components, as expected.

Table XVIII. Budget

Date	Payee	Category	Description	Inflow	Outflow	Balance
	Balance Forward					0.00
1/14/2015	Junior Design Team 1	Income	Junior Design Budget	150.00		150.00
1/14/2015	Junior Design Team 1	Income	SURF Grant	600.00		750.00
3/20/2015	Digi-Key	Electrical	PCB Components for 3 Boards		93.00	657.00
3/20/2015	Digi-Key	Shipping	PCB Components for 3 Boards		7.17	649.83
3/20/2015	OSH Park	Electrical	3 Printed Circuit Boards		43.85	605.98
4/16/2015	Lowe's	Housing	Aluminum and silicone caulk		14.93	591.05
4/16/2015	RadioShack	Housing	Rubber insulated standoffs		3.44	587.61
4/16/2015	Protocol Computer Services	Housing	Thermal compound		8.75	578.86
4/18/2015	Amazon.com	Housing	Waterproof aluminum box		13.09	565.77
4/27/2015	Amazon.com	Electrical	2 Chassis-Mounted 6 Ohm Resistrs		9.17	556.60
4/30/2015	Amazon.com	Packaging	Cardboard box		5.38	551.22
5/1/2015	RadioShack	Electrical	Linear regulator		3.99	547.23

The Bill of Materials is shown in Table XIX. Two important constraints set at the beginning of the project were that prototyping cost must not exceed $150 and production cost must not exceed $75. As shown, the prototyping cost for a single board was $87.21, well within the constraint set. The production cost for a 1000-unit run was calculated to be $40.71, also well within the constraint set.

Table XIX. Bill of Materials

					PROTOTYPE		*PRODUCTION*	
QTY	**CATEGORY**	**DESCRIPTION**	**MAN**	**MAN P/N**	**Unit Cost**	**Cost**	**Unit Cost**	**Cost**
1	DC-DC Converter	120 µH Fixed Inductor	Bourns Inc.	1140-121K-RC	$7.65	$7.65	$5.65	$5.65
1	DC-DC Converter	56 µH Fixed Inductor	Bourns Inc.	2310-V-RC	$3.19	$3.19	$1.77	$1.77
1	DC-DC Converter	27 µF Aluminum-Polymer Capacitor	Nichicon	PLV1J270MDL1TD	$2.53	$2.53	$1.29	$1.29
1	DC-DC Converter	3.3 µF Ceramic Capacitor	TDK Corporation	FK16X7R1E335K	$0.45	$0.45	$0.13	$0.13
1	DC-DC Converter	Schottky Diode	STMicroelectronics	STPS10L60D	$1.78	$1.78	$0.53	$0.53
1	DC-DC Converter	N-Channel MOSFET	NXP Semiconductors	BUK6507-75C,127	$2.05	$2.05	$0.96	$0.96
1	DC-DC Converter	4 Position Terminal Block	On Shore Technology	OSTTC040162	$0.79	$0.79	$0.41	$0.41
2	Sensors	5 mΩ Current Sensing Resistor	Stackpole Electronics Inc.	BR3FB5L00	$0.87	$1.74	$0.31	$0.62
1	Sensors	470kΩ Resistor	Stackpole Electronics Inc.	CF18JT470K	$0.10	$0.10	$0.01	$0.01
1	Sensors	11kΩ Resistor	Yageo	CFR-50JB-52-11K	$0.10	$0.10	$0.01	$0.01
1	Sensors	47kΩ Resistor	Yageo	CFR-50JB-52-47K	$0.10	$0.10	$0.01	$0.01
1	Sensors	1.1kΩ Resistor	Yageo	CFR-50JB-52-1K1	$0.10	$0.10	$0.01	$0.01
1	Controller	IC MCU 16BIT 16KB FLASH 20DIP	Texas Instruments	MSP430G2553IN20	$2.80	$2.80	$1.40	$1.40
1	Controller	IC REG LDO 3.3V 0.8A TO220AB	STMicroelectronics	LD1117V33	$0.62	$0.62	$0.21	$0.21
3	Controller, Sensors	0.1 µF Ceramic Capacitor	Kemet	C410C104M5U5TA7200	$0.25	$0.75	$0.06	$0.19
1	Controller	10 µF Ceramic Capacitor	TDK Corporation	FK18X5R0J106M	$0.40	$0.40	$0.11	$0.11
1	Controller	47 kΩ Resistor	Vishay BC Components	PR01000104702JR500	$0.37	$0.37	$0.05	$0.05
1	Controller	20 Pin DIP Socket	On Shore Technology	ED20DT	$0.26	$0.26	$0.12	$0.12
2	Sensors	Current Shunt Monitor	Texas Instruments	INA271AIDR	$2.44	$4.88	$1.01	$2.03
2	Sensors	1 nF Ceramic Capacitor	Vishay BC Components	S102K29Y5PN63J5R	$0.25	$0.50	$0.05	$0.10
1	Indication	3mm Green LED	Lite-On Inc.	LTL-4236N	$0.33	$0.33	$0.06	$0.06
6	Indication	120 ohm Resistor	Stackpole Electronics Inc.	RNMF14TC120R	$0.14	$0.84	$0.01	$0.09
1	Sensors	IC OPAMP GP 30MHZ RRO 8DIP	Linear Technology	LT1630CN8#PBF	$6.53	$6.53	$3.27	$3.27
3	Sensors	IC MCU 16BIT 16KB FLASH 8DIP	Assmann WSW Components	A08-IC-TT	$0.18	$0.54	$0.09	$0.27
1	Sensors	15uF Capacitor	TDK Corporation	FK24X5R0J156M	$0.45	$0.45	$0.13	$0.13

1	Header Pins	20 Pin Headers	Harwin Inc	M20-9992046	$0.62	$0.62	$0.32	$0.32
1	Packaging	Duck Brand Self-Locking Mailing Box	Duck	1062959	$5.38	$5.38	$1.26	$1.26
1	Housing	BOX ALUM 4.53X3.54X2.17" NAT	Bud Industries	AN-1304	$13.09	$13.09	$8.91	$8.91
4	Housing	Cable Glands	Arlington	LPCG50	$2.11	$8.44	$1.86	$7.44
4	Housing	Rubber insulated standoffs			$0.89	$3.56	$0.02	$0.08
1	Housing	1/16 in. thick, 1 in. wide aluminum			$0.15	$0.15	$0.05	$0.05
1	Housing	Thermal Compound #5	Arctic Silver, Inc.		$1.25	$1.25	$0.25	$0.25
1	Housing	Clear Silicone Caulk			$0.25	$0.25	$0.05	$0.05
1	PCB	Printed Circuit Board	Oshpark.com		$14.62	$14.62	$2.92	$2.92

VI. Future Work Improvements

While this prototype met most of the design requirements which were laid out for it, there are areas where the design could improve. The primary way in which this design could be improved is by increasing the efficiency of the DC-DC converter. Initially the design parameters called for an efficiency of at least 85%. It was found that this parameter was unrealistic for an initial prototype, however for future designs the efficiency of the converter could be boosted by replacing the diode in the Ćuk converter with a second MOSFET, adding a snubber circuit in parallel with each of the MOSFETs, and decreasing the switching frequency of the circuit. By replacing the diode with a MOSFET, the voltage drop across this switch will be significantly reduced and thus decrease the power dissipated by this switch for the same current. Adding a snubber circuit across the MOSFETs would also increase efficiency by reducing the overlap of the current and voltage waveforms at switch transitions which reduces the power dissipated by the switch. Finally, decreasing the switching frequency will decrease the number switch transitions, thus reducing the power losses which result in each transition. Reducing the switching frequency will also allow for more duty cycle steps which will allow for finer resolution in determining the maximum power point of the PV panel.

In addition to increasing the efficiency of the DC-DC converter and increasing the resolution of the MPPT, increasing the power rating of the MPPT is of prime concern. While a 65W MPPT was a good prototype and proof of concept, increasing the power rating of the MPPT will make it a more useful product for users. In order to increase the power rating components with higher current and voltage ratings will need to be used as well as a PCB which can handle more current.

The improvements to the housing would all pertain to ease of use. The PCB can be designed for a specific enclosure where the mounting holes line up with enclosure mounting. The enclosure, though it comes from a large distributor at a cheap price, could be a little bit larger to allow input and output cables to be easily attached to the circuit terminals. Different circuit terminals could also be used in the circuit that allow for wider holes and easier clamping onto cables. Additionally, smaller cable glands that are able to waterproof and clamp 2mm diameter cables within a decent margin should replace the ones currently being used. This does not bring up the issue of whether or not the input cable will be two DC cables in power transmission or two DC cables separately. A solution for this includes offering two different models: one with two cable glands and one with four cables glands. Finally, the side of the enclosure which dissipates heat from the MOSFET and diode should be ground evenly to provide a flat surface for the heat spreader to attach to. The method used on the current model involved a dremel tool with a sanding bit and left a bumpy surface. The thermal grease filled in the rough and bumpy surface, but a lot was required to do so. All in all, the flatter the plane between surfaces, the easier it is for heat to flow from one to the other.

Finally, in order to verify the power rating of the MPPT, additional testing should be done with panels with power ratings higher than 15W. This testing was not able prior to publication date due to time restraints and weather patterns.

VII. Conclusions

In conclusion, this design processes has resulted in an affordable and functional maximum power point tracker which has been tested with PV panels with ratings as high at 65W. The MPPT has been verified to increase the power output to a resistive load by an average of 35.24%. The MPPT design includes an custom Ćuk converter with an efficiency of approximately 75%, and a custom designed printed circuit board which is rated to handle up to 10 A of current. The MPPT uses the Perturb and Observe algorithm to find and track the maximum power point of the PV panel. Additionally, the MPPT is housed within a die-cast aluminum case which is weather resistant and robust. This housing also provides the circuit with excellent thermal performance and is able to keep the circuit below its maximum temperature rating of 185 °F. All of these features were accomplished for a prototyping cost of $87.21 and an anticipated production cost of $40.71 for a run of 1000 units.

Overall this design exceeded expectations and met both the technical and financial requirements which were placed on it. The design is however still in the prototype stage. Areas for improvement for this design include increasing the efficiency of the DC-DC converter, decreasing the switching frequency, increasing the power rating of the design, and replacing expensive components such as the OP-AMP and linear regulator with cheaper alternatives.

VIII. Reflection

In reflecting on this design process, it is first interesting to note the best and worst aspects of our design process. The best design practices that our team developed were detailed research, debugging and problem solving skills, and flexibility. At the beginning of the the design process our team began with lengthy period of research. This research allowed us to understand the inner workings of maximum power point trackers and DC-DC converters, as well as tips for best practices when designing current and voltage sensors. This research allowed us to create a well working design on our first try by learning from the experience and mistakes of others. Our team also developed important debugging and problem solving skills through this project. While our design was very good, it was not perfect, and debugging was necessary. Circuit debugging can be a long and arduous task, but our team work tirelessly to identify issues and find creative solutions. This brings us to the last skill that our team excelled at in this design which is flexibility. When problems arose in the design the team did not just give up, but instead was flexible and willing to change the design in order to improve it. This is extremely evident in the stamps which were created to fix issues

with the original PCB. The next time that we are asked to solve a problem, these are skills and habits that we will implement again.

Our team was not perfect however, and many issues kept this design from being as good as it could be. One of this issues was communication, especially between the electrical and mechanical sides of this project. There was a tendency in our team for the Electrical Engineers to work on the electrical part of the design and not communicate effectively with the Mechanical Engineer, and vice versa. Procrastination was another issue which held back this team. While the team began this project strong and was able to get a working prototype early, procrastination on some key elements including testing, housing, and documentation led to a time crunch in the last few days of the project. The next time we are asked to solve a problem this are issue which we will work to resolve.

It is next interesting to reflect on the positive and negative parts our our design. The overall design was excellent and met or exceeded nearly all the requirements placed on it. One of the positive aspects of the design was the DC-DC convert. This subsystem exceeded expectations in both efficiency and performance. The success of this subsystem was primarily do to the time which went into selecting the design and components for the DC-DC converter. This process included extensive simulations and calculations, as well a sizeable amount of time spent selecting components to meet the required specifications while keeping costs low.

The most negative part of the design was the errors made in the printed circuit board. These errors required the creation of stamps which connected the pins of the integrated circuits to the correct holes in the PCB. These error were made because of procrastination primarily. Too much time was spent researching, which resulted in a rush to submit the PCB design before spring break. This did not leave our team enough time to triple check everything on the board.

From the processes our team has learned that with hard work and a great education anything is possible. We have learned the importance of sharing responsibility and relying on another. We have also learned to identify each other's strengths and assign task based on those strengths. Finally, we have learned how to work in an interdisciplinary team to accomplish a task which could not be done by only Electrical Engineers or only Mechanical Engineers.

APPENDIX A

```
#include <msp430.h>
#include <stdio.h>
//definitions

#define step_size 1
#define PWM_freq 160            //set frequency to 100 kHz
#define TOP_DUTY 128            //set max duty cycle to 80%
#define BOTTOM_DUTY 32          //set min duty cycle to 20%
#define MAX_CURR 5.0            //set max curr to 5 A
#define DELAY 15              // 0.5*(12000/4)
#define TIMER_ON    TA1CTL=TASSEL_1+MC_1+ID_2 // use ACLK, timer on, divide by 4
#define TIMER_OFF   TA1CTL=TASSEL_1+MC_0+ID_2 // use ACLK, timer off, divide by 4

// Global Variables
unsigned int adc[32][4] = {0};         //array to store adc values
float curr_in = 0;              //variable to store current in
float volt_in = 0;              //variable to store voltage in
float curr_out = 0;             //variable to store current out
float volt_out = 0;             //variable to store voltage out

unsigned int duty_cycle = 80;       //variable to store duty cycle, default to 50%

typedef enum {inc, dec} direction;           //enumeration to handle increasing and decreasing
                                             //state for P&O algorithm
direction dir = inc;
unsigned char updown = 1;           // 0 is down, 1 is up
volatile float vo = 0;
volatile float io = 0;
volatile float po = 0;

//Function Prototypes
void Setup_MSP(void);           // Setup watchdog timer, clockc, ADC ports
void Setup_ADC(void);           // Setup input channels and sequences,
void Setup_PWM(void);                       // Setup output pin, PWM freq, initial duty cycle,
                                            // PWM mode, and clock setup
void Read_ADC(void);            // This function reads the ADC and stores values
void PandO(void);                           // function which adjusts duty cycle via the Perturb
                                            // and Observe Algorithm

int main(void)
```

```
                        {
    Setup_MSP();                //settings for the MSP in general
    Setup_ADC();                //settings for ADC
    Setup_PWM();                //settings for PWM
    while (1)
    {
        Read_ADC();             //read values from ADC
        PandO();              //update duty cycle as needed using P&O algorithm
    }
}

void Setup_MSP(void)
{
      WDTCTL = WDTPW + WDTHOLD;             // Stop WDT
      BCSCTL1 = CALBC1_16MHZ;             // Set range
      DCOCTL = CALDCO_16MHZ;          // Set DCO step and modulation
      __enable_interrupt();           // enable all interrupts
}



void Setup_ADC(void)
{
    ADC10CTL1 = INCH_3 + CONSEQ_3;      // A3/A2/A1/A0, multi sequence
    ADC10CTL0 = ADC10SHT_3 + MSC + ADC10ON + ADC10IE + REFON + SREF_1;
    P1DIR = 0;                  // all inputs
    ADC10AE0 |= BIT0 + BIT1 + BIT2 + BIT3; // Disable digital I/O on P1.0 to P1.3
    ADC10DTC1 = 128;                        // 64 conversions
}

void Setup_PWM(void)
{
    P1DIR |= BIT6;                  // PWM output pin
    P1SEL |= BIT6;                  // P1.6 controlled by Pulse width modulation
    TA0CCR0 = PWM_freq;           // PWM Frequency is 150 kHz //200 kHz
    TA0CCR1 = duty_cycle;         // Initial Duty Cycle is 50%
    TA0CCTL1 = OUTMOD_7;          // set/reset mode
    TACTL = TASSEL_2 + MC_1;          // Chooses SMCLK, and Up Mode.
}
```

```
                    void Read_ADC(void)
{
    ADC10CTL0 &= ~ENC;
    while (ADC10CTL1 & BUSY);               // Wait if ADC10 core is active
    ADC10SA = (unsigned int)adc;        // Copies data in ADC10SA to unsigned int adc array
    ADC10CTL0 |= ENC + ADC10SC;             // Sampling and conversion start

    __bis_SR_register(CPUOFF + GIE);        // LPM0, wait for ADC, ADC10_ISR will force exit
    volatile int i = 0;             // variable for for loop
    volatile unsigned int curr_in_sum = 0;
    volatile unsigned int volt_in_sum = 0;
    volatile unsigned int curr_out_sum = 0;
    volatile unsigned int volt_out_sum = 0;
    for (i = 31; i>=0; i--)         //read through all 16 samples of each channel
    {                                           //create a sum of all the samples of each input
for average
       curr_in_sum += adc[i][3];
       volt_in_sum += adc[i][2];
       curr_out_sum += adc[i][1];
       volt_out_sum += adc[i][0];
    }
    //divide each sum by 16 to get the average
    curr_in = (curr_in_sum / 32)*0.01346 + 0.01594;  //equation to calculate curr_in
    volt_in = (volt_in_sum / 32)*0.0661 - 0.27437;   //equation to calculate volt_in
    curr_out = (curr_out_sum / 32)*0.013 + 0.019945;//equation to calculate curr_out
    volt_out = (volt_out_sum / 32)*0.0614 - 0.0524;  //equation to calculate volt_out
}

// ADC10 interrupt service routine
#pragma vector=ADC10_VECTOR
__interrupt void ADC10_ISR(void)
{
   __bic_SR_register_on_exit(CPUOFF);        // Clear CPUOFF bit from 0(SR)
}


void PandO(void)
{
   volatile float p = curr_in*volt_in;     // multiply current x voltage to get power
```

```
                    switch (dir)                // switch based on whether the the duty cycle
                                                // was last incremented or decremented
{
    case inc:               // if incremented
        if (p > po)             // if power has increased
        {
            if (duty_cycle < TOP_DUTY)
            {
                duty_cycle += step_size;  // continue incrementing duty cycle
            }
            else
            {
                duty_cycle -= step_size;  // decrement duty cycle
                dir = dec;
            }
        }
        else if (p < po)          // if power has decreased
        {
            if (duty_cycle > BOTTOM_DUTY)
            {
                duty_cycle -= step_size;  // decrement duty cycle
                dir = dec;          // change direction to dec
            }
            else
            {
                duty_cycle += step_size;  // if power has increased
                dir = inc;          // change direction to inc
            }

        }
        break;
    case dec:                 // if decremented
        if (p > po)               // if power has increased
        {
            if (duty_cycle > BOTTOM_DUTY)
            {
                duty_cycle -= step_size;  // decrement duty cycle
            }
            else
            {
```

```
                                    duty_cycle += step_size;  // if power has increased
                dir = inc;          // change direction to inc
            }
        }
        else if (p < po)            // if power has decreased
        {
            if (duty_cycle < TOP_DUTY)
            {
                duty_cycle += step_size;  // if power has increased
                dir = inc;          // change direction to inc
            }
            else
            {
                duty_cycle -= step_size;  // decrement duty cycle
                dir = dec;
            }
        }
        break;
    }
    TA0CCR1 = duty_cycle;               //update duty cycle
    po = p;                   // store power to compare in next iteration
}
```

REFERENCES

[1] http://ww1.microchip.com/downloads/en/AppNotes/00001521A.pdf
[2] http://www.4pcb.com/trace-width-calculator.html